2F

PNL-2378-3
UC-70

Nuclear Waste Management Quarterly Progress Report July Through September 1978

A. M. Platt
J. A. Powell

January 1979

Prepared for the U.S. Department of Energy
under Contract EY-76-C-06-1830

Pacific Northwest Laboratory
Operated for the U.S. Department of Energy
by Battelle Memorial Institute

Battelle

PNL-2378-3

PACIFIC NORTHWEST LABORATORY
operated by
BATTELLE
for the
UNITED STATES DEPARTMENT OF ENERGY
Under Contract EY-76-C-06-1830

Printed in the United States of America
Available from
National Technical Information Service
United States Department of Commerce
5285 Port Royal Road
Springfield, Virginia 22151

Price: Printed Copy $____*; Microfiche $3.00

*Pages	NTIS Selling Price
001-025	$4.00
026-050	$4.50
051-075	$5.25
076-100	$6.00
101-125	$6.50
126-150	$7.25
151-175	$8.00
176-200	$9.00
201-225	$9.25
226-250	$9.50
251-275	$10.75
276-300	$11.00

PNL-2378-3
UC-70

NUCLEAR WASTE MANAGEMENT QUARTERLY PROGRESS REPORT JULY THROUGH SEPTEMBER 1978

Compiled by
A. M. Platt and J. A. Powell
Nuclear Waste Technology Program

January 1979

Prepared for
the U.S. Department of Energy
Under Contract EY-76-C-06-1830

Pacific Northwest Laboratory
Richland, Washington 99352

FOREWORD

This document is one of a series of technical progress reports designed to report on commercial radioactive waste management programs at Pacific Northwest Laboratory. These programs are funded by the Department of Energy's Office of Nuclear Waste Management. The Commercial Radioactive Waste Immobilization Program is reported elsewhere. These reports are issued on a quarterly basis.

The prior report in this series is Nuclear Waste Management Quarterly Progress Report April Through June 1978, PNL-2378-2.

CONTENTS

LIST OF FIGURES

LIST OF TABLES

1.0 DECONTAMINATION AND DENSIFICATION OF CHOP-LEACH CLADDING RESIDUES

R. L. Dillon, R. S. Kemper, R. R. King

Fuel element cladding residues from the chop-leach head-end process constitute a low-density, high-surface-area metallic waste with a substantial actinide element contamination. The objective of this study is to determine the feasibility of, and to develop methods for, removal of long half-life transuranics from the cladding residues and for consolidation of the zirconium and stainless steel residues. The study involves:

1. *selection and laboratory testing of methods for transuranic removal by*
   - *a) aqueous reagents*
   - *b) molten salt reagents*
   - *c) fluxing during melting*
2. *consolidation of the fuel element hulls by melting and casting Zircaloy, stainless steel, Inconel or alloys of the three*
3. *testing and evaluating the consolidated fuel hulls for long-term waste management*
4. *absorption and fixation of tritium into the waste ingots*
5. *consolidation of transuranics removed.*

SUMMARY

A prototype system for decontaminating and densifying chop-leach cladding residues has been assembled in a building operated by the Pacific Northwest Laboratory. Pilot-scale chemical decontamination equipment and an Inductoslag ingot melting furnace are set up on a simulated hot cell floor plan for eventual combined nonradioactive demonstration. Simulated unirradiated cladding residues will be cleaned in the decontamination prototype, with HF/Ar followed by an aqueous rinse, and then melted in the induction furnace to produce ingots.

The assembled decontamination equipment and associated control equipment are being tested and calibrated.

A melting test of the Inductoslag furnace confirmed that a helium atmosphere could be used during Zircaloy melts; previous tests used argon as the inert atmosphere. Seven ingots from previous melting tests were analyzed and found to meet specifications for metal composition, impurity, and hardness of nuclear-grade Zircaloy.

Five zirconium alloys were compared to Zircaloy-2 sheet material in standard water and steam corrosion tests to examine the effects of alloy composition on corrosion resistance.

The alloy compositions were varied by cleaning, separating, and melting simulated cladding residues to various degrees. It appeared that Zircaloy-4 alloyed with 5 wt% metal additions was less resistant to corrosion than Zircaloy-4 alloyed with 10 wt% and 15 wt% metal additions.

DECONTAMINATION PROCESS

The prototype chemical decontamination equipment consists of an HF gas reactor, an aqueous washer/rinser, plus associated process solution tanks and piping.(1,2) The pilot-scale equipment is designed to decontaminate ∿2 kg cladding/hr. The equipment was completely installed, and all components and control instrumentation are being checked and calibrated. A scrubbed ventilation system is in place to remove any HF gas that might result from minor leaks near the rotating reactor seals. Flow tests showed that simulated, chopped fuel hulls could be transported from the inlet of the HF reactor to the exit of the washer/rinser in a minimum time of 72 min.

DENSIFICATION PROCESS

The basic testing of the Inductoslag ingot melting furnace has been completed. The Inductoslag furnace is the densification portion of the prototype decontamination/densification system. The prototype furnace has been used with a static one-third atmosphere of argon as a protective atmosphere during melting of Zircaloy-4. Twenty Inductoslag furnace heats to melt Zircaloy cladding residues have been described in previous reports.(1,2) Another Zircaloy-4 melting heat (No. 21) was made using helium as a protective atmosphere instead of argon. Table 1.1 summarizes the melting heat. No significant difference was detected between the melting characteristics or visible ingot qualities of ingots melted in the two atmospheres.

During the melting heat in helium atmosphere, the furnace's television monitor did not show a slag ring around the molten metal. It is believed that a change in optical filtering would show the contrast between the slag ring and molten metal that is typically observed when argon is the melting atmosphere.

The alloying elements, impurities, and ingot hardnesses from seven previously melted ingots are shown in Tables 1.2, 1.3, and 1.4 along with the ingot characteristics specified by the American Society for Testing and Materials (ASTM) for nuclear-grade

TABLE 1.1. Inductoslag Furnace Melting Heat No. 21: Zircaloy-4 Melted in a Helium Atmosphere

Heat Number	Melted Weight, kg	Melt Rate, kg/hr	Approximate Power, kW	Energy Use, kWh/kg	Remarks
21	20	41	114	2.8	Melted in helium atmosphere. Slag ring not visible in TV monitor. Need different optical filtering; all other melting and ingot appearances the same as with argon.

TABLE 1.2. Alloy Element Analysis of Inductoslag-Melted Zircaloy-4

Alloy Element	Specified by ASTM - B-350, wt%	Composition of Inductoslag Melting Heats, wt%						
		6[a]	8	9	10	11	15	17
Tin	1.20 to 1.70	1.55	1.47	1.47	1.47	1.50	1.42	1.47
Iron	0.18 to 0.24	0.217	0.205	0.207	0.203	0.204	0.188	0.202
Chromium	0.07 to 0.13	0.117	0.106	0.110	0.105	0.106	0.100	0.109
Fe + Cr + Ni	0.28 to 0.37	0.335	0.312	0.318	0.309	0.311	0.289	0.312

---

a. Inductoslag melting heat number.

TABLE 1.3. Impurity Analysis of Inductoslag-Melted Zircaloy-4

Impurity	Maximum Specified by ASTM B-350, ppm	Composition of Inductoslag Melting Heats, ppm						
		6[a]	8	9	10	11	15	17
Aluminum	75	< 75	< 75	< 75	< 75	< 75	< 75	< 75
Boron	0.5	< 0.2	< 0.2	< 0.2	< 0.2	< 0.2	< 0.2	< 0.2
Cadmium	0.5	< 0.3	< 0.3	< 0.3	< 0.3	< 0.3	< 0.3	< 0.3
Calcium	<100	<100	<100	<100	<100	<100	<100	<100
Carbon	270	160	170	150	200	120	170	160
Cobalt	20	< 5	< 5	< 5	< 5	< 5	< 5	< 5
Copper	50	< 20	< 20	< 20	< 20	< 20	< 20	< 20
Fluorine		14	56	36	36	25	38	37
Hafnium	100	<100	<100	<100	<100	<100	<100	<100
Hydrogen	25	18	23	20	23	17	20	16
Oxygen		1160	1300	1220	1210	1220	1260	1150
Lead		< 5	< 5	< 5	< 5	< 5	< 5	< 5
Magnesium		< 10	< 10	< 10	< 10	< 10	< 10	< 10
Manganese	50	< 10	< 10	< 10	< 10	< 10	< 10	< 10
Nickel	70	< 10	< 10	< 10	< 10	< 10	< 10	< 10
Nitrogen	65	50	50	50	40	40	50	50
Silicon	120	70	80	70	70	70	70	80
Thorium		< 4	< 4	< 4	< 4	< 4	< 4	< 4
Titanium	50		< 20	< 20	< 20	< 20	< 20	
Tungsten	100	< 40	< 40	< 40	< 40	< 40	< 40	< 40
Uranium	3.5	< 1	1	2	1	2	2	1
Vanadium		< 20	< 20	< 20	< 20	< 20	< 20	< 20

---

a. Inductoslag melting heat number.

TABLE 1.4. Ingot Hardness of Inductoslag-Melted Zircaloy-4

		Determined for Inductoslag Melting Heats						
Ingot Hardness	Specified by ASTM B-350	6[a]	8	9	10	11	15	17
Brinell hardness	200	185	189		185	186		184

---

a. Inductoslag melting heat number.

Zircaloy. All the ingots met the required ASTM B-350 ingot specifications. A maximum concentration of fluorine impurity is not specified in ASTM B-350. A previous fluorine analysis of Zircaloy cladding melt stock was 7 ppm. These results indicate that the CaF_2 slag may be adding 7 to 50 ppm fluorine to the melted ingots.

The corrosion resistance of zirconium alloys made from fuel cladding residues affects the potential leachability of the alloy ingots. The particular alloy made from waste cladding depends on the degree of cleaning and separation and on varying manufacturing parameters which produce too many alloys to reasonably test every combination. A selection of various alloys produced to date was made on the basis of materials concentrations representative of cladding residues that were 1) separated, 2) separated and cleaned, 3) unseparated, 4) unseparated but only partially melted, and 5) partially separated and partially melted. Initial corrosion tests (400°C, 1500 psi; 360°C, 3000 psi) have been completed, and the results are shown in Table 1.5. Further corrosion testing in groundwaters at various temperatures is in progress.

The weight gain and appearance of samples exposed to the two corrosion conditions indicate that the presence of 0.5% and 1% oxygen from absorbed corrosion product layers had less effect on the short-term corrosion resistance in water than in steam. Alloys 534-8, 534-21, and 534-13 were heterogeneous metals, essentially some unmelted Zircaloy, stainless steel, and Inconel potted in a eutectic alloy. This potted material tended to retain etching solutions at occasional cracked interfaces; a typical white corrosion product was produced at these interfaces. Previous experience with such "acid staining" of Zircaloy indicates that the staining's effects are mitigated with time. Even with the uncertainty of the potted material, it appears that 5% alloy (534-21) is less corrosion resistant than the 10% alloy (534-14) or the 15% alloy (534-8).

REFERENCES

1. A. M. Platt, compiler, Nuclear Waste Management Quarterly Progress Report, January through March 1978. PNL-2378-1, Pacific Northwest Laboratory, Richland, WA, August 1978.
2. A. M. Platt, compiler, Nuclear Waste Management Quarterly Progress Report, April through June 1978. PNL-2378-2, Pacific Northwest Laboratory, Richland, WA, August 1978.

TABLE 1.5. Comparison of Various Zirconium Alloys Corrosion-Tested in Steam and Water

		Weight Gain During Corrosion,[c] mg/dm^2		
Alloy #	Alloy Type[a,b]	Steam (400°C, 1500 psi, 72 hr)	Water (360°C, 3000 psi, 13 days)	Remarks
--	Unmelted standard Zr-2 sheet	14.8 - 15.3	15.3 - 15.7 - 16.0.	Typical black shiny
431	Zircaloy-4	20	15	Typical black shiny analyses 0.3% O_2
529-18	Zircaloy-4 + 0.5% O_2	29	19	All black--some dull areas
529-12	Zircaloy-4 + 1% O_2	77	20	Black with few small white streaks on steam test
9-5-74	85% Zircaloy-4 10% Stainless Steel 304 5% Inconel 718	59	109	Dull--dark grey (completely melted in graphite crucible)
534-8	85% Zircaloy-4 10% Stainless Steel 304 5% Inconel 718 ∿0.5% O_2	43	48	Dull--rough--dark grey (not completely melted)
534-21	95% Zircaloy-4 5% Inconel 718 ∿0.5% O_2	181	135	Light grey--rough--several white spots and streaks (not completely melted)
534-13	90% Zircaloy-4 10% Inconel 718 ∿0.5% O_2	80	81	Medium grey--rough--white streaks at some potted metal interfaces (not completely melted)

---

a. All alloys except Zr-2 sheet and 9-5-74 were "Inductoslag" melted ingots.

b. Percentages given are weight percent.

c. Samples etched in 39 vol% HNO_3-4 vol% HF before exposure.

2.0 MONITORING METHODS FOR PARTICULATE AND GASEOUS EFFLUENTS FROM WASTE SOLIDIFICATION PROCESSES

R. W. Goles - Project Manager

The objective of this program is to develop reliable and accurate techniques for process monitoring and stack emission monitoring for future waste solidification facilities.

SUMMARY

Process line modifications have been completed, and deployment of the sampling network has begun. Operational testing of laboratory-based equipment has been done.

SAMPLING SITE

All necessary modifications to the process off-gas line, POG-88, required by this monitoring program were completed during this reporting period. Sampling lines were run from POG-88 to Room 147 of the 324 Building, where they were linked to a previously installed gas handling manifold. Installation of sampling network components also began during this period.

LABORATORY PREPARATION

We sampled background levels of selected isotopes of interest and successfully analyzed them in the laboratory. This exercise served not only to establish baseline values for certain important radionuclides, but also allowed operational problems to be solved prior to the actual sampling campaign. This work indicated adequate analytical capability and sensitivity for these isotopes.

3.0. TRU WASTE IMMOBILIZATION PROGRAM

C. R. Palmer - Project Manager

The objectives of this program are to determine the degree of immobilization that may be necessary for the acceptable disposal of transuranic waste residues, and to develop product and process technologies to provide such immobilization.

SUMMARY

Several transuranic waste residues were identified as candidates for application of high-level waste immobilization technology, and chemical compositions were developed for these residues. Laboratory-scale experimental programs were designed to: a) develop near-term borosilicate glass formulations for use in process development; b) develop a generic predictive model for glass component/performance characteristics relationships; and c) evaluate the feasibility of sintered and ceramic waste forms for these residues. Preparation for borosilicate glasses was begun, and preliminary characterization data for sintered ceramics were obtained.

WASTE CHARACTERIZATION - D. K. Davis and C. R. Palmer

The chemical compositions of several transuranic waste residues were defined during the reporting period; these will serve as the initial basis for experimental immobilization studies. These residues, shown in Table 3.1, are generally the result of incinerating typical combustible trash. They were obtained from the literature or from communications with those developing the particular waste handling system. The plutonium-contaminated soil composition labeled Z-9 is also included in the listing. Ash compositions are highly dependent upon the mixture of combustibles as well as the incinerator design and operating conditions, but this collection of data illustrates some typical constituents and the variability in composition that an immobilization system must accommodate.

Secondary wastes from decontamination of metal surfaces using electropolishing techniques were identified and semi-quantitatively characterized. An acid processing system for electrolyte recovery will generate a highly concentrated solution of metal phosphates, the cations being those metals removed from the decontaminated surface. Fixation of this waste in a phosphate glass matrix will be studied next fiscal year.

GLASS DEVELOPMENT - C. W. Griffin, G. B. Mellinger and L. A. Chick

Initial experiments to develop borosilicate glasses for several

TABLE 3.1. Compositions of Transuranic Waste Residues, wt%

Component	RFP Blend(1)	RFP Alpha(1)	Mound	PNL(2)	RFP Heel(3)	SRL	Z-9(4)
Al_2O_3	24.0	35.0	32.7	17.0	4.2	15.0	11.2
B_2O_3					1.6		
BaO					0.3	1.0	
C	3.3	5.0		13.8	28.0	3.0	(a)
$CaCl_2$				3.6			
CaO			6.2	5.5	3.4	24.0	2.5
$CaSO_4$				1.6			
Cr_2O_3	5.5	10.0	2.5		1.7		
CuO	2.3		0.1		0.3		
FeO							6.1
Fe_2O_3	0.5		5.0		6.2	11.0	
H_2O	1.4			4.6			(a)
K_2O					0.3		1.1
KCl				1.3			
MgO	3.4		8.2		1.3	6.0	2.4
MnO_2					0.1		
$NaCl$	2.6	5.0		1.8			
Na_2CO_3	15.5	30.0					
Na_2O	0.8				0.6		2.4
Na_3PO_4	2.1						
Na_2SO_4	2.7	5.0					
NiO			5.5		0.5		
PbO					0.3		
P_2O_5					1.2		
PuO_2					2.5		680 mg/ℓ
SiO_2	36.0	10.0	30.5	34.2	43.0	16.0	55.4
TiO_2			5.8	16.6	3.0	18.0	1.7
ZnO			3.3			6.0	
TOTAL	100.1	100.1	99.8	100.0	99.6	100.0	95.8

---

a. Reported as "volatiles," 13 wt% loss on ignition at 700°C; primarily H_2O and degraded organic solvents.

incinerator ashes have begun and will follow two strategies. The first will be to develop glass frits which will produce final glasses of chemical composition similar to the previously developed high-level waste glass 76-68.(5) Tentative frit compositions are shown in Table 3.2. Performance characteristics will then be evaluated for each waste glass system to determine the degree of immobilization achieved. Resulting glass formulations will subsequently be used to demonstrate the applicability of large-scale high-level waste vitrification equipment to low-level transuranic wastes.

The second experimental strategy will be more fundamental in nature. This approach will involve preparation of a generic series of glasses and determination of their performance characteristics using a statistically designed experimental matrix. These data will then be mathematically modeled in an attempt to quantitatively relate component concentration to dependent performance parameters, such as leach resistance, homogeneity, etc. The predictive value of such a model will greatly enhance the development of future waste glasses. The eleven glass components which will be parametrically studied are shown in Table 3.3, and the range of variability is indicated.

SINTERED CERAMICS - J. M. Rusin and R. A. Wheeler

Two simulated waste compositions, Rocky Flats Plant (RFP) Blend and RFP Alpha (see Table 3.1; compositions were modified slightly to make use of reagent chemicals readily available), were selected to evaluate the feasibility of immobilizing such wastes as sintered ceramics. Pellets about

TABLE 3.2. TRU Frit Compositions

	Concentration, wt%						
	Frit 1 (RFP Blend)	Frit 2 (RFP Alpha)	Frit 3 (Mound)	Frit 4 (PNL)	Frit 5 (RFP Heel)	Frit 6 (SRL)	Frit 7 (Z-9)
SiO_2	38.1	64.7	46.1	57.3	32.8	57.2	20.9
B_2O_3	26.7	17.2	19.6	15.3	21.4	16.7	28.1
Na_2O	7.0	-	25.8	19.4	32.0	22.0	31.3
CaO	5.6	3.6	1.6	-	-	-	-
TiO_2	8.3	5.4	-	-	0.9	-	4.9
ZnO	14.1	9.1	6.8	8.0	13.2	4.1	14.8
TOTAL	99.8	100.0	99.9	100.0	100.3	100.0	100.0
Waste Loading, wt% of final glass	64.4	44.8	51.6	37.8	62.2	43.1	66.2

TABLE 3.3. TRU Waste Glass Components and Constraints, Based on Final Composition Approximating Waste Glass 76-68

Component	Constraints, mole % Lower	Upper
SiO_2	42	58
B_2O_3	6	12
Na_2O	11	16
MgO	0	8
CaO	2	14
Al_2O_3	2	15
TiO_2	2	7
Cr_2O_3	0	3
Fe_2O_3	0	3
NiO	0	3
ZnO	0	6

1.6 cm (0.63 in.) dia by 1.3 cm (0.50 in.) long were formed by cold pressing at 1.4 x 10^8 Pa (20,000 psi), followed by sintering for 2 hr at various temperatures.

Four series of samples were studied for each waste composition:

1. no additives
2. glass frit additive*
3. silica additive (-200 mesh)
4. clay additive (bentonite).

The selected additives may improve the durability of the final waste form in these ways:

- increase sintering by providing a vitreous phase (e.g., SiO_2 reactions to form glass)
- increase consolidation by providing a low-temperature matrix (e.g., coat particle with glass)
- produce stable crystalline phases (e.g., reaction of clay with waste).

Sintering characteristics were evaluated by comparing weight loss and shrinkage/expansion of the sample during sintering. Results for RFP Blend are shown in Table 3.4 and for RFP Alpha in Table 3.5.

When fired without additives, both waste compositions exhibited considerable weight loss, and both expanded at lower temperature sintering schedules. The RFP Blend did demonstrate some shrinkage at 1000°C, and the RFP Alpha also shrank at 1100°C.

Use of additives generally produced more acceptable pellets. In general the silica and bentonite (clay) additions produced the best pellets but required higher temperatures. The frit was limited to 700 and 800°C because of excessive melting and bloating (bubbles and expansion caused by reactions) at higher temperatures. The best pellets produced at 700 and 800°C were from the RFP Blend-frit mixture. RFP Alpha mixtures did not improve the sintering below 800°C.

Condensation of a vapor phase (probably chromium) was observed on the RFP Alpha silica mixtures except for the 66% silica mixture fired at 1100°C. This pellet visually appears to be the best of that series. The RFP Alpha bentonite series produced good pellets except at 1100°C, where excessive bloating was observed.

The RFP Blend-silica and RFP Blend-bentonite series both produced acceptable pellets. Again, some bloating and cracking were observed at 1100°C.

---

* PF 630® (-200 mesh), the O. Hammel Company, Carnegie, PA 15106.

Continuation of this program will involve measurement of density and determination of crystalline phases by x-ray diffraction (XRD). Candidate pellets will be selected from each series for further characterization by leach, volatility, and impact tests.

TABLE 3.4. Sintering Data for RFP Blend

	Sintering Temperature, °C at Temp. 2 Hr									
	700		800		900		1000		1100	
Additive	% Δ Wt	% Δ Ht	% Δ Wt	% Δ Ht	% Δ Wt	% Δ Ht	% Δ Wt	% Δ Ht	% Δ Wt	% Δ Ht
No Additive	-10.6	+4.3	-10.9	+2.7	-11.8	+ 2.0	-12.5	- 5.6	-12.5	melted
50% Frit	N.D.[a]	-2.6	- 7.3	-2.7	N.D.	- 5.3	melted	melted	melted	melted
67% Frit	N.D.	-6.0	- 5.5	-9.4	N.D.	+12.4	melted	melted	melted	melted
50% Silica	- 6.1	+1.0	- 6.3	-2.9	- 6.8	- 2.5	- 7.0	-29.6	- 7.1	0
67% Silica	- 6.3	+0.8	- 6.1	-2.3	- 6.8	- 3.1	- 7.1	-30.6	- 7.0	-3.4
50% Bentonite	-11.2	N.D.	-11.8	+0.3	-12.0	- 0.4	-12.4	+27.6	-12.7	-3.8
67% Bentonite	-10.9	-1.8	-11.5	-1.2	-11.6	- 4.7	-12.1	N.D.	-12.1	-5.7

a. N.D. - Not Determined

TABLE 3.5. Sintering Data for RFP Alpha

	Sintering Temperature, °C at Temp. 2 Hr									
	700		800		900		1000		1100	
Additive	% Δ Wt	% Δ Ht	% Δ Wt	% Δ Ht	% Δ Wt	% Δ Ht	% Δ Wt	% Δ Ht	% Δ Wt	% Δ Ht
No Additive	-15.8	+8.1	-16.0	+5.6	-11.8	+7.3	-18.4	+7.7	-20.0	-15.3
50% Frit	N.D.[a]	-4.7	- 9.3	melted	melted	melted	melted	melted	melted	melted
67% Frit	N.D.	-3.5	- 6.8	+6.3	melted	melted	melted	melted	melted	melted
50% Silica	- 7.7	+3.0	- 9.3	-5.1	- 9.2	-8.3	- 9.4	-6.5	-10.2	+34.5
67% Silica	+ 1.2	-4.7	- 1.5	-5.1	- 0.5	-5.8	- 6.6	-9.6	- 0.8	- 7.2
50% Bentonite	-13.9	+0.9	-14.2	+0.9	-14.7	-1.1	-15.1	+0.9	-15.4	+ 2.3
67% Bentonite	-12.7	+0.3	-13.6	0	-13.8	-5.1	-13.8	N.D.	-14.3	+14.4

a. N.D. - Not Determined

REFERENCES

1. D. L. Ziegler, et al., Status Report: Waste Incineration and Fixation for Waste Management, Production and Reprocessing Division of the Department of Energy, July-December, 1976. RFP-2655, Rockwell International Atomics International Division, Rocky Flats Plant, Golden, CO, November 25, 1977.

2. L. K. Mudge, R. A. Walter and G. F. Schiefelbein, Waste Treatment and Handling Processes, Annual Report. BNWL-1861, Pacific Northwest Laboratory. Richland, WA, September 1974.

3. T. C. Johnson, Recovery of Plutonium from Incinerator Ash at Rocky Flats. RFP-2520, Rockwell International Atomics International Division, Rocky Flats Plant, Golden, CO, December 21, 1976.

4. M. J. Kupfer, et al., Glass Forms for Alpha Waste Management. ARH-SA-239, Atlantic Richfield Hanford Company, Richland, WA, July, 1975.

5. W. A. Ross, et al., Annual Report on the Characterization of High-Level Waste Glasses. PNL-2625, Pacific Northwest Laboratory, Richland, WA, June, 1978.

4.0 KRYPTON SOLIDIFICATION

G. L. Tingey - Project Manager

The objective of this program is to develop alternative techniques for storing radioactive krypton in a solid matrix. Two techniques are currently being investigated: dissolution of krypton in low-density glass followed by densification at high temperature and entrapment of the krypton in solids during ion sputtering.

SUMMARY

Release of krypton from sputter deposited amorphous $Fe_{.87}Y_{.13}$ shows a mechanism similar to that of high-temperature release. Release of ^{85}Kr from a metal sample was calculated to be 0.07% of the ^{85}Kr released in 100 years at 200°C and 12% released in that period at 300°C. This krypton retention should be more than adequate for radioactive krypton storage.

Krypton solubility measurements in low-density glass under 347 atm. pressure of krypton heated to 840°C and held for 4 hr show krypton contents from 2 to 3 cm^3 of Kr(STP)/gm of glass. These loadings now appear to be sufficient for krypton storage. Furthermore, preliminary measurements of the release characteristics of such samples indicated even better retention than observed for the sputter-deposited metals.

KRYPTON ENTRAPMENT DURING SPUTTERING - G. L. Tingey, M. A. Bayne, E. D. McClanahan and P. J. Raney

We have demonstrated earlier that krypton gas can be trapped in sputter-deposited metal matrices. As reported in a previous quarterly report,(1) sputter-deposited amorphous metals may contain higher than 10 at.% krypton. Krypton release measurements have also been reported(2) which showed two types of release, one attributed to normal diffusion through the metal and a second which released at low temperatures more rapidly than expected from the diffusion mechanism.

During this quarter we have measured the long-term low-temperature release rate of a sample of krypton loaded 87% iron, 13% yttrium which sputtered as an amorphous metal. In this study the sample was held at various temperatures for several days and the release rates determined as a function of time. It was observed that the initial, relatively high rate was transitory and would decrease with time to an apparent steady-state rate after several hours. The steady-state rates appear to agree well with the extrapolated rate from the higher temperature release, and are thus considered to be releasing via the same mechanism as at high temperature. The release rates of the sample are shown in Figure 4.1. This rate is plotted as a function of temperature and fits the equation:

$$\frac{d[Kr_R]}{dt} = 345e^{-27,000/RT}[Kr_{(s)}] \qquad (1)$$

where $d[Kr_R]$ is the krypton release rate of the sample at temperature T in units of moles of krypton released per minute. R is the gas constant and has the value of 1.987 calories/mole/degree. $Kr_{(s)}$ is the moles of krypton contained in the sample.

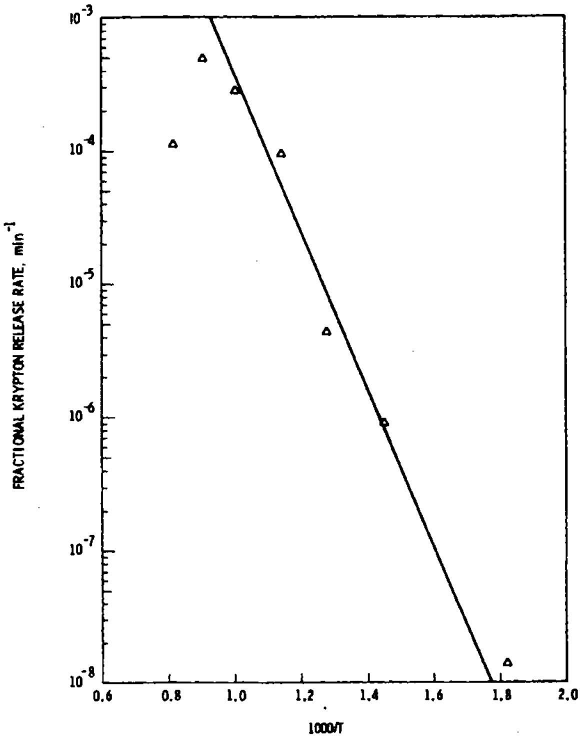

FIGURE 4.1. Krypton Released from a Sample of Sputter-Deposited $Fe_{\cdot 82}Y_{\cdot 12}Kr_{\cdot 06}$ as a Function of Temperature

It is of interest to determine the extent to which radioactive krypton (^{85}Kr) would be released from a sample over a long time, taking into account the decay of the ^{85}Kr. The ^{85}Kr concentration in a sample at any time, t, can be expressed by the equation:

$$^{85}Kr_{(s)} = {}^{85}Kr_{(s)_0}\ e^{-\lambda t} \qquad (2)$$

where $^{85}Kr_{(s)}$ is the moles of ^{85}Kr in the solid at time t, $^{85}Kr_{(s)_0}$ is the moles at t = 0, and λ is the radioactive decay constant equal to 1.22×10^{-7} min.$^{-1}$. Substitution of equation 2 into equation 1 and integration with respect to time from 0 to t yields the expression

$$\frac{^{85}Kr_R}{^{85}Kr_{(s)_0}} = 345e^{-27,000/RT}\left[\frac{1}{\lambda} - \frac{e^{-\lambda t}}{\lambda}\right]. \qquad (3)$$

Using the expression the fraction of ^{85}Kr released during time t can be calculated for any sample temperature. For example, 0.07% of the ^{85}Kr would be released after 100 years from a sample held at 200°C, and 12% would be released if the sample temperatures were maintained at 300°C for 100 years.

Although these data are somewhat preliminary, they show more than adequate krypton retention properties for storage of ^{85}Kr for the long term.

KRYPTON DISSOLUTION IN LOW-DENSITY GLASS - W. J. Gray, G. L. Tingey and K. R. Wheeler

Krypton dissolution in low-density glasses followed by sintering of the glass to prevent rapid release of the krypton was studied at near 1 atm krypton pressure and reported in a previous quarterly report.(3) These experiments showed a satisfactory krypton content, but the long extrapolation to useful pressures (∿2000 atm.) provided the incentive to study the dissolution at higher pressures. During this quarter, we have dissolved krypton in a low-density SiO_2-based glass and in a lower melting glass. These samples were heated at a rate of about 200°C/hr to 840°C at a pressure of 347 atm. krypton and held at this temperature for 4 hr to densify the samples. The samples were then cooled under pressure and krypton release measurements performed in vacuum as a function of temperature.

The SiO_2 glass contained 2.16 cm^3 of Kr(STP)/g of SiO_2 and released less than 1% of the krypton below 600°C. The low-melting glass was densified more completely than the SiO_2, yet it contained 2.97 cm^3 of Kr(STP)/g of glass and retained 99.95% of the krypton to 890°C.

If the krypton solubility is considered to be linear to 2000 atm., the krypton content would be 12.5 and 17.1 cm^3 of Kr(STP)/g of glass for the SiO_2-based and the low-melting glass, respectively. These loadings appear satisfatory for storage of the krypton. Furthermore, based on the release characteristics measured, release of krypton in glass appears to be even lower than that observed in metal matrices. Further studies are required to determine the long-term, low-temperature release behavior of these samples.

REFERENCES

1. M. A. Bayne, E. D. McClanahan, G. L. Tingey, E. N. Greenwell, and R. W. Moss, "Krypton Entrapment During Sputtering." Nuclear Waste Management Quarterly Progress Report January Through March 1978, PNL-2378-1, August 1978.
2. M. A. Bayne, E. D. McClanahan, G. L. Tingey, E. N. Greenwell, and R. W. Moss, "Krypton Entrapment During Sputtering." Nuclear Waste Management Quarterly Progress Report April Through June 1978, PNL-2378-2, November 1978.
3. W. J. Gray and G. L. Tingey, "Krypton Dissolution in Low-Density Glass." Nuclear Waste Management Quarterly Progress Report January Through March 1978, PNL-2378-1, August 1978.

5.0 CARBON-14 AND IODINE-129 FIXATION

L. L. Burger - Project Manager

The objective of this program is to develop and demonstrate the technology needed to safely and effectively immobilize ^{129}I *and* ^{14}C *released from treatment of irradiated fuels.*

SUMMARY

Significant factors influencing the iodate leach rate from Portland type III cement have been statistically isolated from 17 factors screened in a Plackett Burman Screening Analysis. Temperature, CO_2 concentration in the leachate, and concentration of fixation material, cation common to the fixation material and silver nitrate in the cement matrix showed the more consistently significant effects.

A system was constructed and tested for loading iodine onto metal-exchanged zeolites and recycling the zeolite by stripping off the loaded iodine with hydrogen. Results comparable with previously reported studies were obtained.

Additional tests on iodide-iodate conversion were conducted to evaluate oxidation and to determine the effect of hydroxide concentration on ozone oxidation of iodide. The electrolytic method converted 98% of the iodide to iodate. Preliminary results indicate that hydroxide concentration affects the final oxidation state of iodine in an ozone environment.

LEACHABILITY STUDIES - K. D. Wiemers

One method of immobilizing ^{129}I involves conversion to some stable, insoluble solid compound of iodine followed by incorporation of the compound in Portland cement. To evaluate the feasibility of this storage form, tests on the leachability of iodine from cement are being conducted. Previous reports(1,2) have described the results of Phase I and the experimental parameters of Phase II of the leachability studies. The following discussion describes the results of Phase II, a 17 factor x 28 trial Plackett Burman Screening Analysis.(3) In this analysis the effect which cement composition, leachate composition, and fixation material had on the leach rate of iodate from cement were investigated.

To determine the effects of the 17 factors studied as a function of time, the iodate leach rate was tabulated daily. With the initial amount of iodate in the Specimen, A_o, the incremental amount of iodate leached, a_n, the specimen's geometric volume, V, surface area, A, and weight, M, and the leach period, t_n, all known, the values shown in Table 5.1 were computed

TABLE 5.1. Leach Data Computed

Description	Symbol	Units
Cumulative amount iodate leached	Σa_n	mg I
Cumulative fraction iodate leached	$\frac{\Sigma a_n}{A_o}$	dimensionless
Normalized cumulative fraction iodate leached	$\frac{\Sigma a_n}{A_o} \frac{V}{S}$	cm
Incremental leach rate	$\frac{a_n}{A_o} \frac{M}{S} \frac{1}{t_n}$	$\frac{g}{cm^2/day}$
	$\frac{a_n}{A_o} \frac{V}{S} \frac{1}{t_n}$	$\frac{cm}{day}$

for each trial. The incremental leach rate, cm/day, was selected as the dependent variable for the statistical analysis because it was independent of prior leach data and normalized for both the volume and surface area of the specimen. The Plackett Burman screening design was applicable to the data from the first 15 days of leaching. A programmable calculator was used to perform the statistical computations.

In the statistical analysis a value for each factor effect was computed daily. Ranking the effect values from largest to smallest established the relative importance of the factors. Reported are all of the factors obtained by selecting the top five factors from these daily rankings. These factors were retained for further evaluation as recommended for the Plackett Burman screening procedure.(3) Ranked factors which were statistically significant at a 95% confidence level were temperature, concentration of carbon dioxide and sulfate in the leachate, and concentration of fixation material, silver nitrate, bentonite, aluminum chloride, and cation common to the fixation material in the cement matrix. The remainder of the ranked factors, which were not statistically significant, were fixation material solubility, concentration of calcium in the leachate, concentration of barium in the cement matrix, application of a commercial dressing or sodium silicate coating, and curing time. Figure 5.1 provides a representation of the relative importance of these factors as a function of time. The most consistent effects were observed with temperature, concentration of CO_2 in the leachate, concentration of the fixation material, cation common to the fixation material, and silver nitrate in the cement matrix, as described below:

- Increasing temperature increased the leach rate of iodate from the cement matrix. This effect was greatest during the first 7 days of leaching. The temperature levels in this study were ambient and 75°C.
- Increasing the concentration of CO_2 in the leachate decreased the leach rate of iodate. The effect was largest during the first 9 days. The initial concentration levels for CO_2 in the leachate were 0 and 0.04 M.

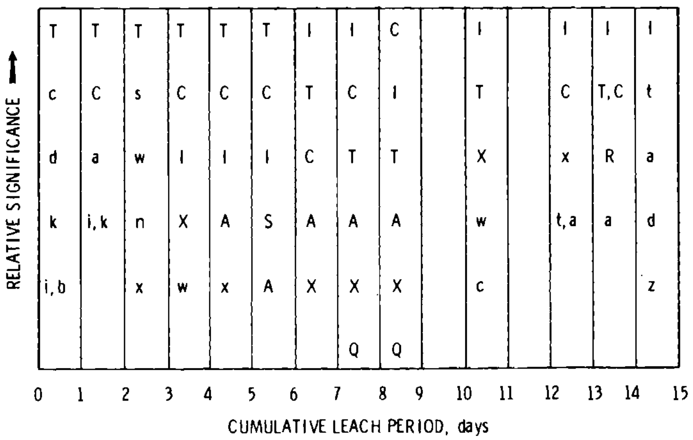

KEY FOR FIGURE 5.1

SYMBOL	FACTOR	SYMBOL	FACTOR
A,a	[Ag$^+$] CEMENT	Q	[AlCl$_3$] CEMENT
B,b	[Ba^{+2}] LEACHATE	R	[BENTONITE] CEMENT
C,c	[CO$_2$] LEACHATE	S,s	[SO$_4^{2-}$] LEACHATE
D,d	COMMERCIAL DRESSING	T,t	TEMPERATURE
I,i	[IO$_3^-$] CEMENT	W,w	[Ca^{+2}] LEACHATE
K,k	SOLUBILITY FIXATION MATERIAL	X,x	CONCENTRATION IN CEMENT OF CATION COMMON TO FIXATION MATERIAL
N,n	SODIUM SILICATE COATING		
		z	CURING TIME

CAPITAL LETTERS - FACTORS SIGNIFICANT AT A 95% CONFIDENCE LEVEL

FIGURE 5.1. Significant Factor Effects

- Increasing the concentration of fixation material in the cement sample increased the leach rate. The effect was greatest after the third day. Concentration levels were 0.137 and 0.686 mmole iodate/g cement.
- Adding silver nitrate to the cement matrix decreased the leach rate of iodate. The effect became significant after 4 days. Concentration levels were 0 and 0.014 mmole silver ion/g cement.
- Adding to the cement matrix a cation common to the fixation material did not result in the predicted retardation. Between the fourth and thirteenth leaching days cation addition increased the leach rate. The levels of cation addition were 0 and 0.686 mmole cation/g cement.

The remaining factors had effects which were either of short duration or of irregular occurrence. Solubility of the fixation material was important during the first 2 days of leaching: iodate leach rate increased with increasing solubility of the fixation compound. Concentration of calcium in the leachate was important during the third, fourth, and eleventh leach days: increased concentration of calcium in the leachate increased the leach rate. Ranked factors showing no obvious trend were concentration of barium and bentonite in the cement matrix, application of commercial dressing or sodium silicate coating, concentration of sulfate in the leachate, and curing time.

Although the data were presented as if each factor were isolated, interpretation of the real cement/iodate leaching system should consider each factor as an integral part of the total system. Explanation of the effects of the more important and consistent factors observed will be discussed in a topical report. The following comments on these effects are largely conjecture. In these comments a positive effect corresponds to an increased leach rate, and a negative effect to a decreased leach rate.

The positive effect of temperature on the leach rate of iodate from a cement matrix is consistent with solubility, diffusion, and cement stability phenomena.(4) Further study is required to define the mechanisms. Evidence suggests that regulation of temperature during leach studies is important and that temperature criteria may need to be established for ^{129}I storage in cement.

The negative effect of CO_2 concentration in the leachate on the leach rate of iodate from cement may result from pore-filling or coating actions of carbonate salts. These results suggest that a carbonate pretreatment for cement containing the iodine fixation form may reduce the iodate leach rate and thus provide a more stable storage form.

The positive effect of iodate concentration on the leaching of iodate from cement suggests that a compromise may be required between the resistance to leaching and the amount of fixation material encapsulated.

Addition of silver nitrate to the cement matrix causes a negative effect on the iodate leach rate. This indicates that silver ions may trap free iodate resulting from solubility and/or exchange processes. The effectiveness of this factor warrants further investigation.

The addition of common cation to the cement matrix caused an unexpected effect on the leach rate of iodate. This may be due to interference of the excess ions of the salt with the cement curing process.(4) This effect demonstrates the interaction of the cement system with basic leaching phenomena. It suggests the need to avoid adding large amounts of ions uncommon to the cement matrix.

From the leach data collected in this study specific values can be extracted and compared with previously performed leach tests. By the fifteenth day of leaching, 0.02 to 2.05 wt% of the iodate had been leached from the specimens and the incremental leach rate for that day ranged from 0 to 2.23×10^{-3} cm/day. Values for similar iodate leach rate expressions extracted from data collected by Oak Ridge National Laboratory (ORNL) were in the range of 0.44 wt% and 2.4×10^{-2} cm/day.(5) The differences between the ORNL values and the lowest values obtained in the screening test support the concept of decreasing the leach rate by optimizing the most influential factors.

Future studies to be conducted include:

- extended-time leach study to establish predictability curves for extrapolation to long-term storage
- a response surface analysis to establish predictability curves for temperature, concentrations of CO_2 in the leachate, and concentration of fixation material and silver nitrate in the cement matrix.
- screening test to determine factors affecting the leach rate of iodide fixation materials in cement
- screening test to determine factors affecting the leach rate of carbonate fixation materials in cement.

IODINE TRAPPING - K. D. Wiemers

A system was constructed and tested for loading iodide onto metal exchanged zeolites followed by recycling of the zeolite bed by regeneration with hydrogen. This work was the initial phase in continuing the extensive tests of different metal-exchanged zeolites for trapping iodine from dissolver off-gas performed at the Idaho National Engineering Laboratory (INEL).(6,7) Future work includes studies of both the characteristics of methyl iodide loading onto reduced metal zeolites and various stripping techniques. The data described below are to provide a reference point for these investigations.

The iodine loading apparatus was described in a previous report.(2) In the iodine stripping system nitrogen and 100% hydrogen were plumbed to the reaction vessel to purge the system with nitrogen and then replace the nitrogen with hydrogen. The influent gas was preheated in a U-tube and passed into the bottom of the reaction vessel. This arrangement provided an iodine stripping operation countercurrent to the iodine loading process. The hydrogen iodide in the effluent was trapped with 0.1 N NaOH scrubbers. A coldtrap downstream from the scrubbers removed water from the effluent to prevent condensation's forming in the exhaust flowmeter. An iodide-specific ion electrode was used to analyze the scrubber solutions. This analytical method had a detection limit for our collection system of 2.5 ppb HI (g) by volume.

Studies of the flow rate and column dimensions indicated that the iodine loading capacity could be significantly increased over those previously reported(3) by using a 10-cm bed depth. At this depth the iodine loading capacity at room temperature face velocities of 5.1 and 15 m/min did not vary significantly. Reproducibility of the INEL iodine loading and stripping data(1,2) provided the acceptance criteria for these parameters.

The testing conditions for both the iodine loading and iodine stripping processes are given in Table 5.2. Silver-exchanged (18.2%) mordenite, Agm, in the form of 1/16-in. extrudates was used in this study.

The results for the iodine loading are best discussed in terms of the instantaneous decontamination factor as a function of loading capacity (Figures 5.2 and 5.3). The curves begin at a loading capacity corresponding to the minimum time required to

TABLE 5.2. Experimental Conditions

	Iodine Loading		Iodine Stripping
Run order[a]	1	3	2
Dry bed wt, g	45.0	(b)	(b)
Bed diameter, cm	2.5	2.5	2.5
Bed depth, cm	10.0	10.0	10.0
Bed temperature, °C	150	150	500
Carrier gas	Air	Air	Hydrogen
Face velocity, m/min	5.1	5.1	5.1
Average I_2 concentration, g/m^3	2.0	1.5	0.0
Average H_2O (g) concentration, %	7	7	0
Pretreatment	(c)	(d)	(e)

---

a. The Agm was exposed to the following sequential runs: 1) iodine loading, 2) iodine stripping, and 3) iodine reloading.

b. To maintain distribution of mordenite material, the weight was not determined prior to these runs.

c. The Agm was exposed to air containing 7% H_2O at a flow rate of 2.5 ℓ/min for 23 hr at 150°C.

d. Mordenite material was loaded and stripped under given conditions.

e. Mordenite material was loaded with iodine and exposed to dry nitrogen for 2 hr at 300°C.

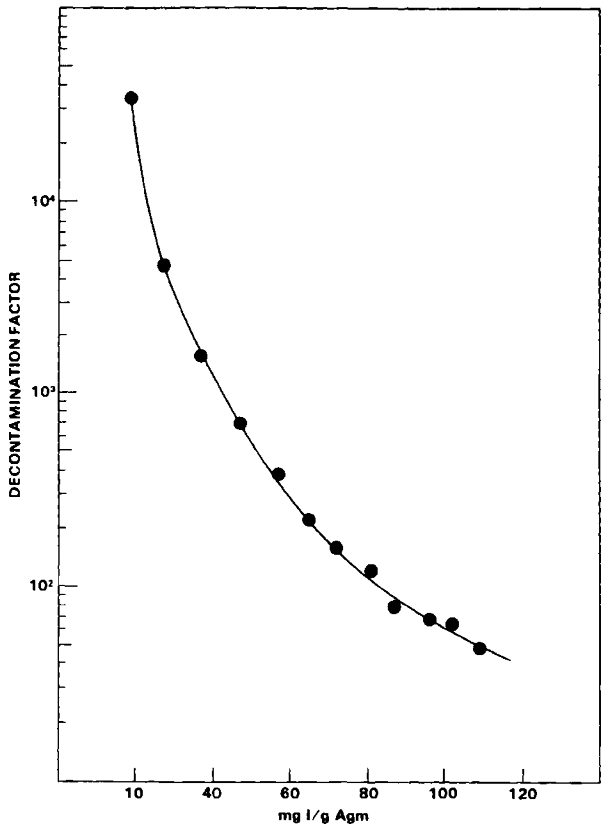

FIGURE 5.2. Run 1: Iodine Loading onto Silver Mordenite

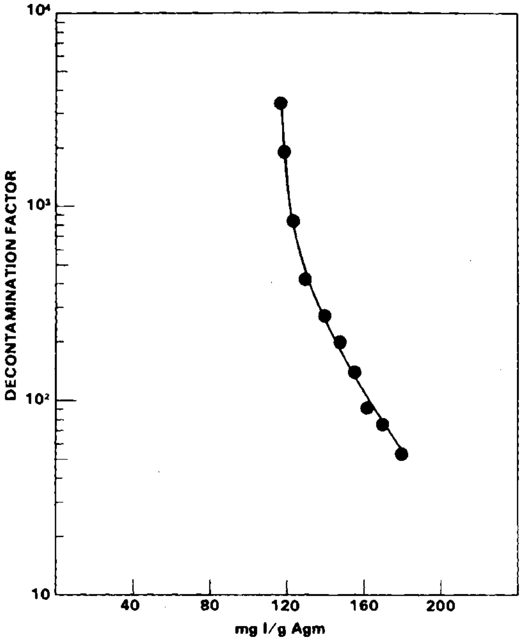

FIGURE 5.3. Run 3: Iodine Loading onto Recycled Silver Mordenite

recover the first effluent sample. Figure 5.3 is shifted to the right because the iodine previously loaded and not stripped was included in the loading capacity. Table 5.3 summarizes these data.

During the first run the silver-exchanged mordenite was loaded to 109 mg I/g Agm. This corresponds to a decontamination factor of 4. The amount of iodine physically absorbed was calculated from the iodine trapped in the caustic scrubber during the nitrogen drying period. During this period 0.6% of the total iodine loaded on the silver-exchanged mordenite was removed. The increase in loading capacity (from 42 to 118 mg I/g Agm at a DF of 10^3) observed during Run 3 may be due to the reduction and/or migration of the silver during the iodine stripping process.(8)

TABLE 5.3. Iodine Loading Results

	Maximum I_2 Loading, mgI/gm Agm	
Run Number[a]	DF>10^3	DF>10^2
1[b]	42	82
3[c]	118	160

---

a. Defined in Table 5.1(a).
b. The Agm used for Run 1 was pretreated with air containing 7% H_2O at 150°C for 23 hr.
c. The Agm used for Run 3 was not removed from the reaction vessel since Run 1. Its "pretreatment" therefore consists of all the previous runs.

The results for the iodine stripping are presented in terms of the desorption rate of hydrogen iodide as a function of the amount of iodine removed from the iodine-loaded silver-exchanged mordenite (Figure 5.4). The average HI strip rate was 2.1 mg HI/min-cm^2, occurring when 27 to 70% of the loaded iodine had been removed from the silver-exchanged mordenite. A sharp decrease in the HI strip rate

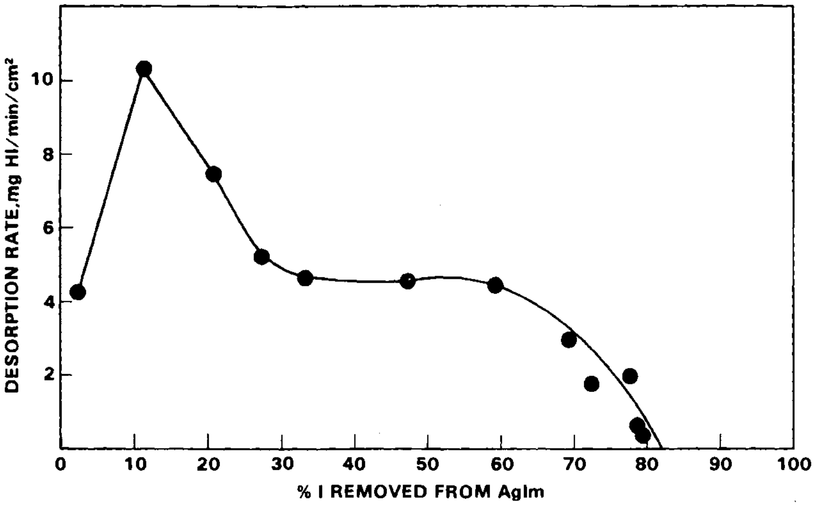

FIGURE 5.4. Run 2: Iodine Stripping from Silver Iodide Mordenite

was observed after 70% of the loaded iodine was removed from the silver-exchanged mordenite. The stripping process was terminated when 80% of the loaded iodine was removed from the silver-exchanged mordenite. The HI strip rate at termination was 0.2 mg I/min-cm^2.

IODIDE TO IODATE CONVERSION - R. D. Scheele

Additional experiments were performed to evaluate electrolytic oxidation of iodide to iodate and to determine the effect of hydroxide concentration on ozone oxidation of iodide.

The electrolysis was performed using a technique similar to that developed by H. H. Willard and R. R. Ralston(9) for conversion of iodine to iodate. In our work the anodelyte was 0.8 $\underline{M}$ HCl and 0.1 $\underline{M}$ KI, and the cathodelyte 2 $\underline{M}$ HNO_3. Platinum disks were used for both electrodes. The electrolysis cell consisted of two compartments separated by a porous Pyrex glass frit. Neither compartment was sparged. The mechanism and reasons for selection of the anodelyte and cathodelyte are discussed by Willard and Ralston.

The cell was operated for 1.6 hr at a current density of 0.1 amp/cm^2. At the end of this period 98% of the iodide was converted to iodate as determined by iodiometric titration; 8% of the iodate was found in the cathode solution. Two oxidation steps were observed: 1) the iodide conversion to iodine and 2) iodine conversion to iodate. During the experiment iodine precipitated out on the anode. Iodine was also present in the vapor above the solution. As the iodine was oxidized, the iodine in the vapor phase redissolved; thus no iodine was lost due to vaporization. Possible methods for retarding iodine volatilization include increasing the HCl concentration and/or operating at lower temperatures.

As mentioned in the previous quarterly report, ozone oxidation of iodide requires a pH >7 to prevent iodine volatilization. The two experiments described here were performed in 0.05 and 0.01 M NaOH. The iodide concentration was 0.1 M. Iodiometric titrations were used for determining the iodide oxidation products. For both experiments the ozone concentration was 4.5 mole % in air. In the first experiment the product was a mixture of iodate and periodate; a white precipitate began forming at an ozone-to-iodine mole ratio of 18. The experiment was terminated at an ozone-to-iodine mole ratio of 90. In the second experiment iodate was the only product formed and no white precipitate formed. Less than 10^{-7} M iodide remained in the second solution, as determined with an iodide-specific ion electrode. This experiment was terminated at an ozone to iodine mole ratio of 64. The preliminary indication is that hydroxide concentration affects the final oxidation state of the iodine.

These experiments and those reported in previous quarterly reports have shown that ozone is an effective oxidant for iodide in a basic solution.

REFERENCES

1. Nuclear Waste Management Quarterly Progress Report January through March 1978. PNL-2378-1, Pacific Northwest Laboratory, Richland, WA, August 1978.
2. Nuclear Waste Management Quarterly Progress Report April through June 1978. PNL-1278-2, Pacific Northwest Laboratory, Richland, WA, November 1978.
3. "Strategy of Experimentation," Applied Technology Division, E.I. duPont deNemours, Wilmington, DE, rev. ed., October 1975.
4. F. M. Lea, The Chemistry of Cement and Concrete, 3rd ed., Chemical Publishing Co., Inc., 1971.
5. W. E. Clark, C. T. Thompson, and W. B. Howerton, Fixation of Radioiodine with Portland Cement, Part I: Preliminary Scoping Studies. ORNL-TM-5064, Oak Ridge National Laboratory, Oak Ridge, TN, 1975.
6. T. R. Thomas, B. A. Staples, L. R. Murphy, and J. T. Nichols, Airborne Elemental Iodine Loading Capacities of Metal Zeolites and a Method for Recycling Zeolite. ICP-1119, Allied Chemical Corporation, Idaho Falls, ID, 1977.
7. T. R. Thomas, B. A. Staples, and L. P. Murphy, The Development of Ag°Z for Bulk ^{129}I Removal from Nuclear Fuel Reprocessing Plants and PbX for ^{129}I Storage. ICP-1135, Allied Chemical Corporation, Idaho Falls, ID, 1977.
8. T. R. Thomas, "The Development of Ag°Z for Bulk ^{129}I Removal from the Nuclear Fuel Reprocessing Plants and PbX for ^{129}I Storage." Proceedings of the 15th Air Cleaning Conference, Boston, MA, August 10-15, 1978.
9. H. H. Willard and R. R. Ralston, "The Electrolytic Oxidation of Iodine and of Iodic Acid." J. Electrochemical Society, 42: 239, 1932.

6.0 INTERNATIONAL PROGRAM COORDINATION

K. M. Harmon - Project Manager

Develop and maintain an information system covering nuclear waste management R&D Programs and technology in other nations, for use by U.S. government agencies and DOE contractors.

Collecting, review, summarizing and cataloging of significant foreign travel reports, technical documents, and other publications continued. Research and reference services were provided to DOE and contractor personnel upon their request.

7.0 WASTE MANAGEMENT SYSTEM STUDIES

J. V. Robinson - Program Manager

The objectives of this program are to evaluate alternative systems for treatment and disposal of radioactive wastes and to develop information required to ensure effective communication with the public.

SUMMARY

A seismicity catalogue was compiled of approximately 5500 earthquakes in the Pacific Northwest. Seismic strain release maps were constructed for the Hanford area, Washington State, the Pacific Northwest, the continental U.S., Alaska, and the world. A map showing all known faults in the State of Washington and another locating all rivers and lakes in Oregon were constructed. Geologic field investigations of a 270-km-long photolineament in the States of Washington and Oregon were completed and preliminary conclusions reached regarding the photolineament's geology.

The feasibility of using kriging to characterize geologic waste repository sites has been demonstrated.

Work was begun in developing a suitable analytical framework for the systematic analysis of waste management issues by an interdisciplinary (technical and nontechnical) team.

Draft reports were completed on print media coverage of nuclear and coal issues; the relationship of human values and attitudes to nuclear power/nuclear waste issues; DOE's communication process; and public attitudes toward waste disposal facilities.

DATA BASE DEVELOPMENT FOR NUCLEAR WASTE MANAGEMENT - H. P. Foote and T. N. Bishop

This work is aimed at providing data and methods to quantitatively address technical factors such as seismic stability that are a concern in licensing and safety analysis procedures for waste repositories.

Present work is developing the data base and computerized capability to manipulate the data for practical applications.

Seismic Data Base

A seismicity catalogue for the Pacific Northwest was compiled this quarter. Our various data bases (primarily National Oceanic and Atmospheric Administration (NOAA); Canada; and Woodward-Clyde) were merged to form a total of 8500 earthquakes in the region of 41°N to 52°N and and 103°W to 135°W. Roughly 3000 duplicate events were subsequently identified and discarded, using the programs AUTO and DOOP. Maps at a scale of 1:500,000 were plotted with symbol size a function of magnitude. These maps, along with the listings of the events in the catalogue, were sent to the Army Corps of Engineers in Seattle for use in their Dam Safety program.

A seismic strain release map was made for the Pacific Northwest using these data. Benioff, in 1952, postulated that strain release, related to fault displacement at the time of the earthquake, is proportional to the square root of its energy release. The energy, E, can be related to surface wave magnitude (M_s) using the equation given by Richter (1958):

$\log_{10} E = 11.4 + 1.5M_s$ where E is in ergs (1)

Often, however, M_s is unknown, and other magnitudes or noninstrumental data such as intensity or felt area must be used to solve for the energy. Using the Pacific Northwest data, the following relations were derived:

$M_s = 1.88m_b - 4.65$ (m_b is body wave magnitude (2)

$m_b = 0.75M_L + 1.28$ (M_L is local magnitude) (3)

$M_s = 1.22 \log_{10}A - 0.50$ (A is felt area in km^2) for events east of 120°W (4)

$M_s = 1.47 \log_{10}A - 1.53$ for events west of 120°W (5)

$M_s = 0.667\ I_o + 1$ (I_o is maximum intensity on the Mercalli scale) (6)

Energy was calculated for each of the earthquakes using equations (1) through (6). Then the appropriate map projection was chosen, a grid system set up, and the energies of the earthquake in each square were summed. The summed energy grid was smoothed, logarithms were taken, the data were contoured and printed on a color-contoured map. The zones of high seismic activity show up well in red and yellow. The most active areas seem to be the Blanco fracture zone, the Gorda Ridge, the Mendocino fracture zone, and the Queen Charlotte Islands fault offshore, and the Puget Sound-Willamette trough and the Rocky Mountains on land.

Additional strain release maps of the Hanford area and of the State of Washington were constructed using microseismic data from 1969-1978. Strain release maps of the continental United States, Alaska, and the world used edited data from the NOAA data base. These strain release maps have been studied carefully, and conclusions will appear in a final report.

Mapping and Geographic Data Base

A composite fault map has been compiled for the State of Washington from five sources:

1. State of Washington Department of Natural Resources Geologic Map of Washington - 1961
2. Geologic studies of Columbia River Basalt Structures and age of Deformation. The Dalles-Umatilla region, Washington and Oregon, Boardman Nuclear Project, Report ID PJB by Shannon and Wilson, Inc., 1973.
3. Washington fault map
4. Geologic Reconnaissance of the Cle Elum-Wallula Lineament and Related Structures, Shannon and Wilson, Inc., 1977.
5. Tectonic map from Shannon and Wilson, Inc., report on WPPSS Nuclear Project units No. 1 and 4, 1977.

The faults were digitized in three categories:

- known faults

- inferred faults
- concealed faults.

These maps provide better coverage in the central and eastern portion of the state than in the west. There is also a range of accuracy and scale represented by this sample of maps. However, many of the better known faults are covered, and the composite map can be upgraded in local areas where the information is available. In making the composite map, duplicate fault coverage was eliminated by retaining what is thought to be the most current and detailed interpretation. Sources 2 and 4 were ranked best, followed by 5, 1 and 3. Figure 7.1 is a plot of the level 1, or known, faults. The remaining levels of faults could be plotted separately or added in different colors.

The compilation of the high-resolution Oregon map from the 1:250,000-scale series USGS maps has been completed. There are two composite files:

File 1: coastlines, lakes,
islands at three levels
of detail
File 2: rivers at four levels of
detail plus canals.

In both files the point spacing corresponds to about 600 ft on the ground. Figure 7.2 is a plot of all river and lake levels for Oregon. Every fifth point was plotted in this case because of the small scale. More of the points would be used for a larger scale map.

Two new computer programs (ERGMAP, ERGPIC) were written to produce the seismic strain release maps. The first program (ERGMAP) reads a binary file containing the earthquake locations and energies. The events are averaged on a grid appropriate to the size of the region considered. The map may be interpolated to a finer spacing and smoothed. Several commonly used projections may be selected for the output map. The second program (ERGPIC) generates the color-coded hardcopy image on the DICOMED digital image recorder. Additionally, the program computes the map scale and other parameters required for the geographic overlay. The overlay map is produced with the main mapping programs as a standard plot file. This file is combined on the DICOMED negative to form the complete map. Any of the available geographic files could be overlayed in this step. For example, the Washington fault map could have been added to the energy release map. The final result is one color negative that may be printed at the desired scale.

We are presently preparing a report on the current status of the GEOMAP system of programs and data bases. It will contain detailed descriptions of the programs and provide examples of the output products produced to date.

GEOLOGIC INVESTIGATIONS IN THE NORTHWEST - G. A. Sandness and W. M. Phillips

The purpose of this research program is to identify and evaluate major photolineaments* in the

---

* A photolineament is an alignment of topographic, tonal, or textural features seen in aerial photographs or satellite imagery.

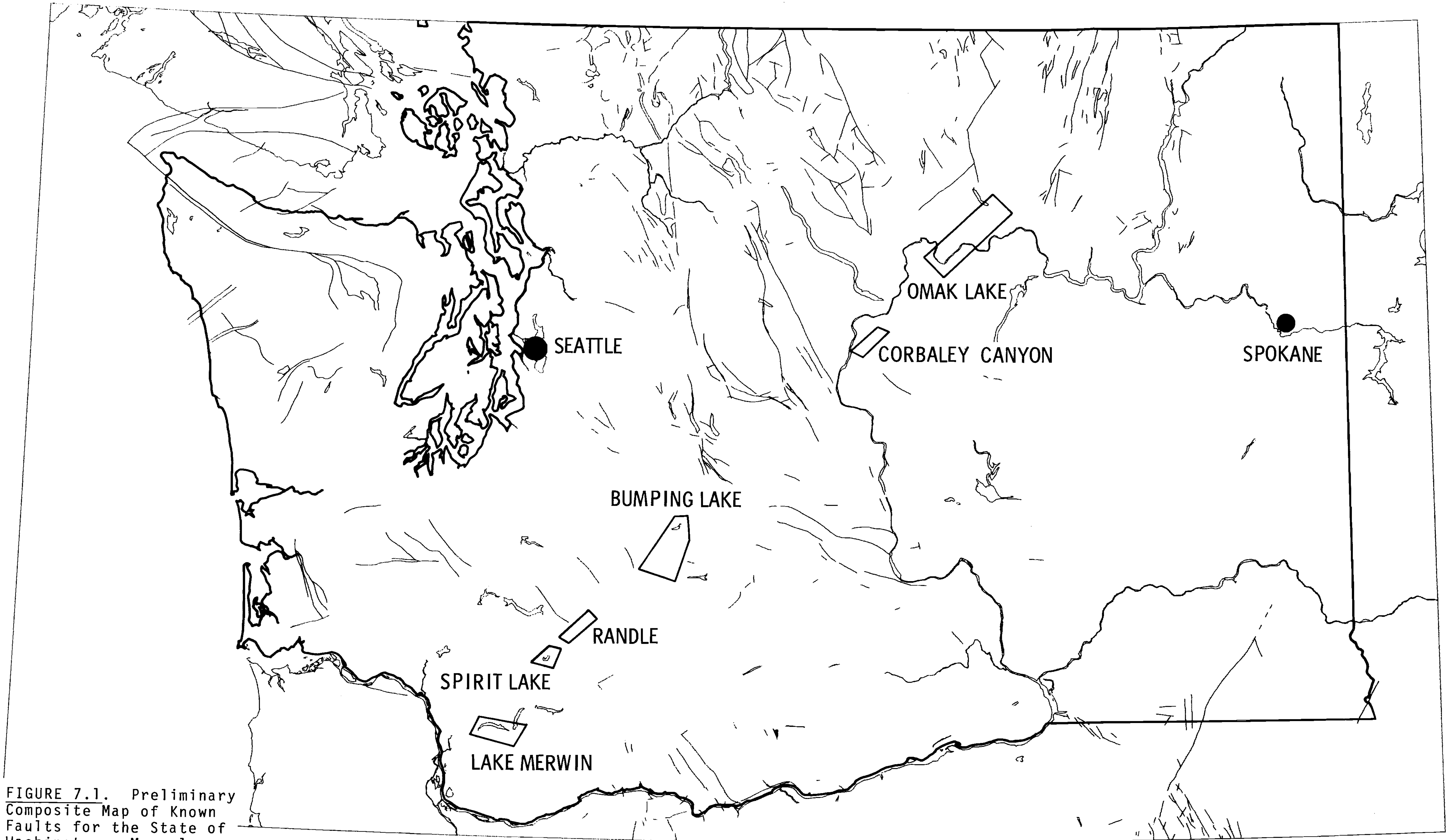

FIGURE 7.1. Preliminary Composite Map of Known Faults for the State of Washington. Map also shows areas of field studies of selected photolineaments.

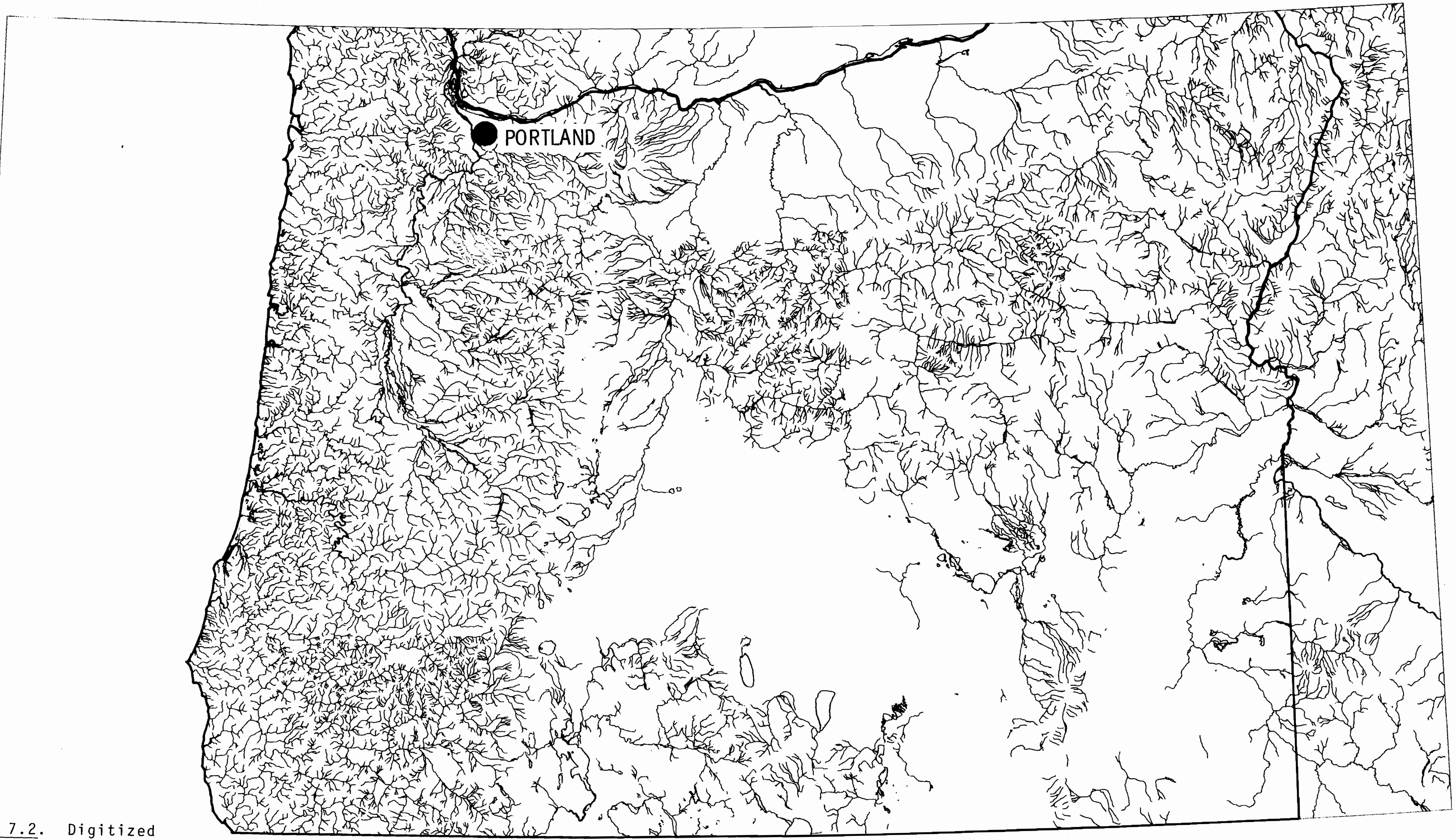

FIGURE 7.2. Digitized Rivers and Lakes for Oregon (116°W to 125°W, 42°N to 46°N)

Northwest. Research was divided into the following primary tasks:

- use of satellite imagery, U-2 aerial photographs, and conventional aerial photographs to identify lineaments to be studied
- collection of existing geological and geophysical data pertinent to lineament studies
- geologic field studies of selected lineaments
- evaluation of collected data.

Based upon analysis of Landsat satellite imagery, augmented by U-2 and conventional aerial photographs, a major NE-SW trending photolineament about 270 km long was identified in the states of Washington and Oregon. The photolineament crosses the Columbia River near Portland, Oregon, and continues NE to a point just east of Omak Lake, Okanogan County, Washington. This photolineament was selected for further study after rock exposure conditions and accessibility were shown, via remote sensing techniques, to be favorable.

Upon selection of the major photolineament, a data base was constructed using the following sources:

- University of Washington and Washington State University M.S. and Ph.D. theses
- publications or open-file reports of the United States Geological Survey
- publications or open-file reports of the Department of Natural Resources, State of Washington
- dam siting reports commissioned by Pacific Power and Light for hydroelectric projects in the central Cascades of Washington
- professional papers published in various geological and geophysical journals.

Computer reference search services were used to insure completeness of the data base. Computer searches were made of all data published between 1967 and the present concerning structural geology, igneous petrology, seismicity, volcanism, sedimentary petrology, and regional geology in the State of Washington. An additional computer search provided listings of current geologic research in the state.

Analysis of the data base indicated that NE-SW trending faults had been previously recognized along two portions of the major photolineament. The two areas, the Bumping Lake area northeast of Mt. Rainier and the Lake Merwin area south of Mt. St. Helens, were selected as sites for geologic field studies.

The data base was also used in conjunction with remote sensing techniques to identify further areas along the trace of the photolineament best suited for productive geologic field studies. As the great length of the photolineament precluded mapping along its entire length, the following criteria were used to select field sites: 1) rock type; 2) degree of expression of the photolineament; 3) amount of previous work done along the photolineament; 4) accessibility.

Preference was given to areas with sedimentary or flood basalt lithologies as their uniform layering allows rapid detection of faults.

However, much of the lineament is best expressed in the volcanic terrain of the central Cascades and in the granitic terrain of the Okanogan Highlands of north central Washington. Several sites for field analysis were thus chosen in those localities where expression of the photolineament, existing previous work, and accessibility were favorable. These areas (shown in Figure 7.1) are:

1. the Lake Merwin area, Cowlitz and Clark counties, Washington
2. the Spirit Lake area, just northeast of Mt. St. Helens, Skamania County, Washington
3. the Randle area, Lewis County, Washington
4. the Bumping Lake area, east and northeast of Mt. Rainier, Lewis and Yakima counties, Washington
5. the Corbaley Canyon area, Douglas County, Washington
6. the Omak Lake area, Okanogan County, Washington.

The first five areas were studied by Battelle geologists from June 1978 to the end of September 1978. Previous work by Battelle geologists in the Bumping Lake area was done in the fall of 1977.

Geologists from Washington State University under direction of Dr. J. W. Mills were contracted by Battelle to study the Omak Lake area during the summer of 1978. Their work was completed this quarter, and a final report has been submitted to Battelle.

A variety of geologic field methods were employed by Battelle. They included detailed photogeologic analysis of geomorphologic features of the study areas, stratigraphic studies of the volcanic and sedimentary rocks present, sampling of fossils, petrologic descriptions of representative lithologies, and mapping of joints, folds, faults, and lithologic contacts.

In-lab research included analysis of fossil pollen from the Bumping Lake area and x-ray fluorescence (XRF) analysis for ten major elements in 50 whole-rock samples collected in the Bumping Lake area. Neutron Activation Analysis (NAA) for trace elements was also performed on five of the whole-rock specimens used for XRF analysis. The fossil pollen analysis was performed by Professor L. H. Fisk at Walla Walla College, Washington, in June 1978. The XRF major element analysis was conducted by Dr. Peter Hooper at Washington State University, and Dr. J. C. Laul of Battelle performed the NAA portion, both during this quarter.

PRELIMINARY CONCLUSIONS

Preliminary conclusions available at the end of the quarter include those of Battelle geologists and those of the Washington State University team:

Lake Merwin Area

Faulting producing small displacements occurs in Tertiary (Eocene-Oligocene?) basalt or basaltic-andesite flows in the Ariel damsite area. The fault traces trend NE-SW and lie on the trace of the photolineament. The time of faulting is uncertain. Undeformed calcite and zeolite veins cross-cutting fault planes indicate that the faults are not presently active.

An apparent structural offset is also present across the trace of the photolineament at the Ariel damsite. East-striking, southerly dipping Tertiary volcanics are present on the east side of the dam. To the west, across Lake Merwin, Tertiary volcanics outcrop with a variety of southeasterly dips.

Photogeologic analysis suggests that NE and NW trending fractures have broken the major structure of the area, an east-west trending anticline, into several parts, rotating large blocks of inclined volcanics into NE-SW striking attitudes. The pattern of structural trends coalesces at TumTum Mountain, about 16 km east of Lake Merwin. TumTum Mountain is a recent basaltic cinder cone. Recent volcanic activity in the area may have been localized at TumTum Mountain by the presence of older (Miocene to Pliocene?) fault zones.

Spirit Lake Area

The trace of the major photolineament corresponds to differential erosion between the resistant Mt. Margaret batholith and surrounding, hydrothermally altered, Eocene to Oligocene volcanics and volcanic clastics. Diffuse zones of chalcopyrite-pyrite-tourmaline-quartz mineralization appear to follow east-west structural trends in the area. Mineralized zones, isolated fault zones, and near-vertical tuff beds appear to reflect deformation related to batholithic intrusion.

Randle Area

A very narrow, extremely straight NE-trending syncline or intracanyon flow in basalts and basaltic-andesites of the Ohanapecosh Formation (Oligocene) was mapped on the trace of the major photolineament in the Iron Creek Butte area. The structure represents a deviation in the general northwesterly structural trends of the region and may be controlled by an Oligocene or older fault zone.

A dike swarm, probably representing an Oligocene volcanic center, was also mapped on Lone Tree Mountain. The trace of the major photolineament is strongly expressed in both the Iron Creek Butte and Lone Tree Mountain areas.

Bumping Lake Area

The region lies on the projected southerly trace of the Straight Creek Fault, a structure recently deemed by WPPSS geologists as probably active. The structure and stratigraphy of the area is complex. Solution of key geologic problems revolves around the ability to define an accurate stratigraphic section in the lithologically monotonous Ohanapecosh Formation. A pilot study aimed at using major and trace element concentrations in the volcanic suite to define a stratigraphic section has been initiated using XRF and NAA technology.

Preliminary results of the XRF pilot study indicate that XRF techniques offer precise means of chemically classifying igneous rocks found in the Bumping Lake area and elsewhere in the Cascades. An example of the methods used to identify and chemically compare rock samples is shown on the variation diagram of Figure 7.3. Standard granite, diorite, and gabbro compositions are plotted on the diagram to delineate general classification fields. Oxide concentrations of analyzed samples are then plotted to establish general compositional limits of the sample population. More sophisticated statistical methods are used to study chemical variation in samples within a single compositional category.

To date, the XRF data have been useful in establishing--or disproving--correlation of rocks possessing similar field characteristics. Analysis of NAA trace element data and more sophisticated study of XRF information will greatly aid in defining the stratigraphic column needed to identify major faults in the Bumping Lake area.

Field evidence independent of the XRF and NAA studies indicates that a geologic discontinuity, either a fault or unconformity, exists in the NE trending Bumping River valley.

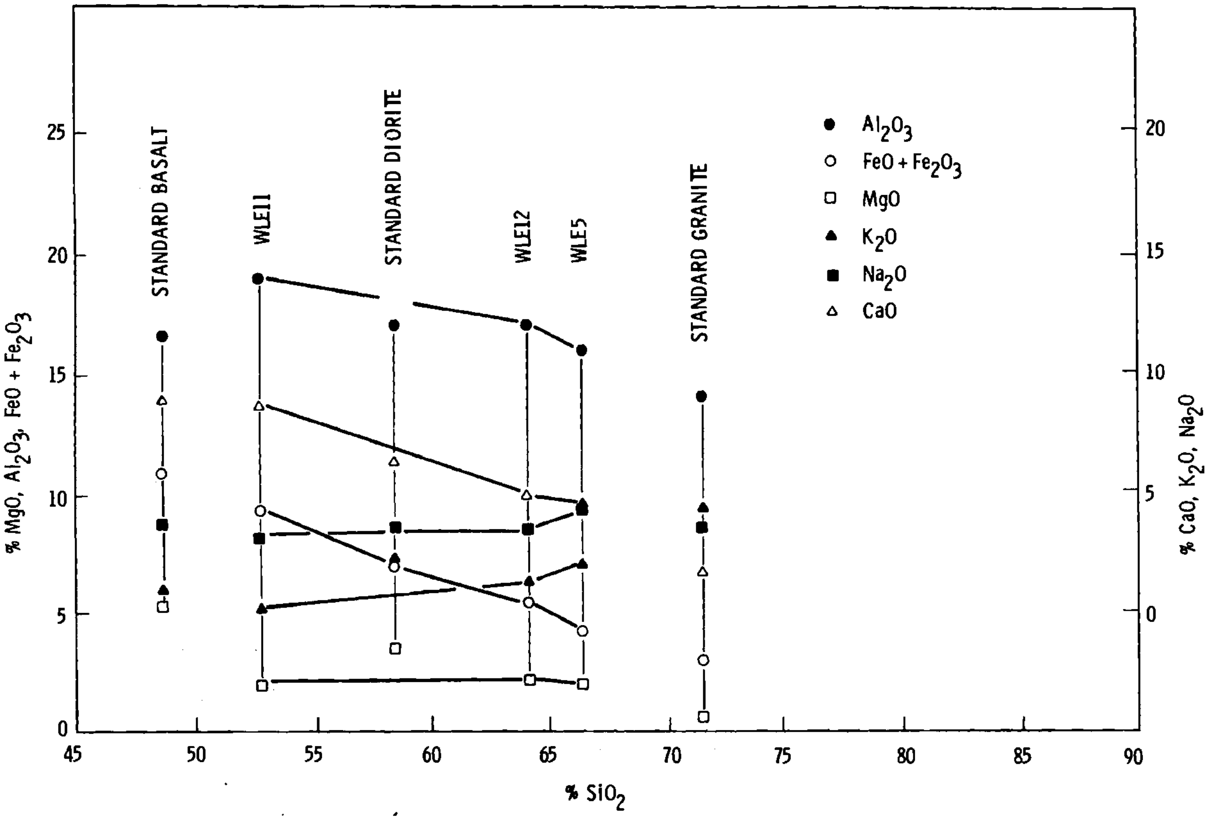

FIGURE 7.3. Variation Diagram Illustrating Use of Major Element Oxide Concentration to Chemically Classify Igneous Rocks from the Bumping Lake Area. Oxide concentrations of three samples are plotted. The samples have similar structural and petrological characteristics in the field, but XRF analysis shows them to be distinct units chemically.

Additional evidence for faulting exists in the Three Lakes, Carlton Pass, and possibly Cortright Creek areas.

Corbaley Canyon

The photolineament is expressed by a narrow, very straight canyon containing only emphemeral drainage. The canyon's NE trend is controlled by strong jointing in the pre-Tertiary metamorphics and Miocene basalts of the area. No evidence for faulting was located in the area.

Omak Lake Area

The region is generally underlain by massive granite of Cretaceous age. A study of the granites exposed to the southeast of Omak Lake, and of the Miocene Columbia Plateau basalts to the southwest, revealed no evidence of major faulting in the direction of the photolineament. Further, no statistical predominance of joint trends in the direction of the photolineament was identified. However, definitive conclusions concerning the nature of the photolineament could not be made because of Quaternary alluvium along the postulated trace of the photolineament in the area southeast of Omak Lake.

Evaluation of the Photolineament

Evidence to date suggests that the major NE-trending photolineament is a complex, composite structure geologically expressed by faulting, folding, igneous activity, and residual strain release structures (joints). Age of the structure is uncertain and is probably composite. Accurate determination associated with the lineament awaits much more detailed mapping in the Washington Cascades together with radiometric dating of key volcanics and intrusives.

Additional information relating to geologic structure, particularly in the Bumping Lake area, will require further field and laboratory studies to examine the possible correlations among rock units in the study areas and to establish improved stratigraphic control on which sound structural interpretations can be based.

KRIGING - P. G. Doctor

The objective of this effort is to evaluate the kriging method for its applicability to the characterization of potential geologic repository sites for storage of high-level radioactive wastes. Kriging is a statistical method for estimating functions which describe spatially distributed phenomena such as groundwater elevation and depth to salt, basalt, or shale deposits.

The study evaluation process is perceived to be a two-stage procedure. The first step is to characterize representative data sets, such as those mentioned above, using kriging techniques. During the last quarter this was accomplished using water elevation and depth to basalt data sets for the Columbia Plateau.

The second step is to observe the behavior of the kriging technique as the number of data points decreases, thereby simulating an actual site-evaluation data set. This was completed in this quarter using the basalt measurements.

The basalt-elevation data set was systematically reduced to observe the effect of fewer data points on the contours estimated by the kriging method. The basalt kriging elevations are quite variable, even over short distances. Contrary to what is intuitively expected, reducing the data set sometimes makes the phenomenon's estimated structure more complex. However, the reduced-data estimates seem to remain within two standard errors of the full-data estimates, and in more than one instance, the reduced data set with a more complex structure led to markedly better estimates than those produced by the full data set.

Another approach for dealing with sparse data that seems to have good application for site selection is co-kriging. Basically, it consists of 1) relating costly measurements (core data) to less costly nonintrusive measurements (perhaps seismic data), 2) estimating core measurements at locations where the other data were taken, and 3) then estimating contours and additional sampling locations from the extended core data. It is a quasi-simulation procedure that could effectively combine different types of information. Pierre Delfiner of the Paris School of Mines has been working on this technique. It is being used successfully to estimate plutonium distribution from in-situ americium measurements in the Eniwetok Atoll clean-up and at the Nevada Test Site.

To resolve certain questions which had arisen during this stage of investigations, P. G. Doctor attended the Paris School of Mines short course on kriging, September 11-22. The course was eminently worthwhile from two standpoints. First, it provided a good overview of geostatistics and its application to spatial phenomena. Many technical questions have been resolved or can now be resolved by referring to the literature. Secondly, interaction with mining and petroleum geologists attending the course has led to an improved perspective of geology, including the types of data available and geostatistical applications.

The overall perspective gained from the course indicates that the work on characterizing the water and basalt elevation data sets has been reasonable. The work on reducing the basalt data set to simulate a sparse data set is of academic interest but of questionable practical value for site characterization.

In reality, although there may be little core data, there are other types of data (e.g., seismic, or knowledge of a fault) to use in combination because a decision on the suitability of a potential site will not rest on the core data alone. Use of kriging to combine different types of data is a sound idea; sparsity of core data is a problem shared with petroleum engineers, and co-kriging has been a valuable approach for them. One case study in the Paris School of Mines course was an example of using seismic and core data to evaluate a potential underground gas reservoir.

The technique for selecting the optimal location of an additional core sample is easily applied. However, its successful application rests on how well the geologic phenomena have been modeled. It seems that the emphasis should be to develop kriging in combination with all existing data to obtain the most complete characterization of the site, and then apply the sample location selection technique.

Although questions of a technical nature remain, kriging has demonstrated its feasibility to characterize geologic waste repositories.

SPENT FUEL STORAGE - A. B. Johnson, Jr.

This program has developed an assessment of spent fuel behavior in water pool storage which includes the following publications by A. B. Johnson, Jr.:

1. Behavior of Spent Nuclear Fuel in Water Pool Storage, BNWL-2256, Pacific Northwest Laboratory, Richland, WA, September 1977.
2. "Impacts of Reactor-Induced Fuel Cladding Defects on Spent Fuel Storage," presented at OECD/NEA Symposium on Spent Fuel Storage, Madrid, Spain, June 20-30, 1978. Published in Conference Proceedings, Storage of Spent Fuel Elements.
3. "Testimony for California Energy Resources Conservation and Development Commission," BNWL-SA-6213, March 10, 1977. Summarized in Summary of Testimony Regarding Spent Fuel Assembly Storage, California Public Resources Code 25524.1, March 10, 1977, Docket Nos. 76-NL-1, and 76-NL-3, issued May 26, 1977.
4. "Spent Fuel Integrity in Water Pool Storage," Am. Nucl. Soc. Trans., 27:488-89, 1977.
5. "Spent Fuel Behavior in Water Pools," PNL-SA-6817. Presented at NRC-IAEA Spent Fuel Storage Meeting, Bethesda, Maryland, February 28-March 2, 1978; published in Proceedings.
6. "Spent Fuel Integrity in Pool Storage," presented at the meeting Back End of the LWR Fuel Cycle, Savannah, Georgia, March 19-23, 1978.
7. "Utility Spent Fuel Storage Experience," PNL-SA-6863, presented at the American Nuclear Society - Executive Conference on Spent Fuel Policy and Its Implications, Buford, Georgia, April 2-5, 1978; published in Conference Proceedings.
8. "Spent Fuel Storage Experience," to be published in Nuclear Technology.

A program is now moving into an experimental stage which will be funded by the DOE through the Away From Reactor Spent Fuel Storage Program Office located at the Savannah River Laboratories.

A. B. Johnson, Jr. will attend an International Fuel Cycle (INFCE) Working Group No. 6 meeting in Vienna in October to provide technical support to the U.S. delegation. Visits to discuss spent fuel storage issues to KWV at Erlangen, Germany, and to Swedish laboratories at Studsvik (Studsvik Energiteknik AB) and Västerås (Asea Atom) also are planned during the trip. The trip will be funded by the DOE AFR program. Development of information for the meeting was done under Battelle's Waste Management Systems Studies support.

A program was scoped to evaluate the long-term (multi-century) behavior of metals. The goal is to assess long-term survival of various metals in a variety of environments so as to determine whether such information is useful in waste management assessments.

ASSESSING NUCLEAR WASTE MANAGEMENT OPTIONS - R. G. Bradley (Teknekron, Inc.)

At the end of the last quarter, work was initiated under a subcontract with Teknekron, Inc., of Washington, DC, on development of a suitable analytical framework for the systematic analysis of radioactive waste management issues by an interdisciplinary team.

Review of attempts to analyze complex issues by interdisciplinary experts has revealed one or more of these disadvantages inherent in the analytical approaches heretofore employed:

- the technical and nontechnical representatives were separated during their analyses
- the unmanageably large size of the groups performing the analyses impeded development of the desired product
- the framework for the deliberations was insufficiently structured and guidelines were inadequately defined to keep efforts focused on achieving the product.

Teknekron has elected to test the conceptual analytical framework by analyzing a waste management issue with a relatively small interdisciplinary team (three technical and three nontechnical personnel). The team will undertake the analysis as a direct and continuous dialogue until the desired product is derived. Moreover, the deliberators will be constrained by ground rules to focus on the issue to be analyzed and the product to be derived without unduly confining the dialogue's scope. They will also be provided in advance concise background material to ensure understanding of the issue and its relation to the physical waste management system considered.

To gain further insight on the applicability of the analytical framework, the subcontractor plans to test it by convening two such small interdisciplinary teams--one constituted from experts within Teknekron and one with participants from other private industrial organizations and universities. Both groups will analyze the same issue and work under the same ground rules administered by a Teknekron panel to be convened first. This should permit a useful iteration of the guidelines and background material before convening the outside panel in October 1978.

While the chief aim for both panels is to perform the systematic analysis of the assigned waste management issue within the structured analytical framework, Teknekron plans to gain certain additional benefits, to the extent feasible, from this collection of expertise. These would include:

- a critique of the analytical framework as a viable tool for analyzing waste management issues
- the experts' views on alternative methodologies for performing such analysis
- identification of what they perceive to be the compelling issues for the acceptability of deep geologic repositories as a long-term waste management/disposal strategy.

<u>NUCLEAR WASTE COMMUNICATIONS</u> -
S. M. Nealey and W. L. Rankin (HARC)

The public's perceptions, attitudes and knowledge about nuclear waste management are highly related to reactions to nuclear power. Our studies have therefore focused on nuclear waste management issues as imbedded in a larger framework of nuclear power and broader energy issues. These perceptions and attitudes have been analyzed through

- news media and government coverage of nuclear power and nuclear waste issues
- public attitudes, knowledge, and values regarding nuclear power and nuclear waste disposal
- public policy issues in nuclear waste management.

In our print media analyses, we have found that:

1. The print media generally have provided a somewhat balanced picture of nuclear power, although certain specific sources such as <u>Environment</u> and the <u>National Observer</u> were antinuclear.
2. Antinuclear stories slightly outnumbered pronuclear stories, possibly leaving a slightly negative influence with readers.
3. Coal issues were treated by these sources more neutrally and less controversially and given less prominence than nuclear issues.
4. Coverage of nuclear issues (especially antinuclear) has increased steadily since 1972, whereas coal coverage peaked in 1974 and has since decreased.
5. Peaks in coverage of nuclear waste issues came in 1974 because of a waste leak at Hanford and again in 1976 as a result of state nuclear power initiatives.

The television analysis, now in the write-up stage, indicates that nuclear power and coal issues have received more prominence than solar issues in the number of news broadcasts and that nuclear power was handled in a more polarized manner, coal in a more neutral, and solar in a positive manner. Television news broadcasts have tended to treat coal and solar more favorably than nuclear power; however, absolutely speaking, nuclear power has not received an exceptional amount of bad publicity.

While the print media and television have increased their coverage, the Federal government has greatly decreased its information flow to the public regarding nuclear power. Underestimating the public's trust in the government to provide unbiased information, DOE has very few brochures available on nuclear power, with only one about nuclear waste (the nuclear issue the public wants most to learn about). These brochures appear uninterestingly written and difficult to read, requiring a college education for understanding.

A survey of Washington residents conducted earlier has resulted in collection of data in two categories: 1) nuclear knowledge as related to nuclear attitudes and 2) the relationship of human values and attitudes to nuclear power issues. Additionally, data from this survey are being analyzed as to whether or not there are sex differences in attitudes regarding nuclear power. This research in knowledge, attitudes, and values relevant to nuclear power indicates that there is no single, simple explanation as to why some people support and some oppose nuclear power. Individual differences on the importance placed on human values, on information and misinformation about nuclear power, and on attitudes about general energy and nuclear-specific issues all influence attitudes about nuclear power. However, human values and knowledge appear to combine to form attitudes about nuclear power, thus making the combination of values and knowledge a central determinant.

Our findings are that the importance one places on the values for a comfortable life, a world at peace, a world of beauty, family security, freedom, and national security is a strong determinant of nuclear power attitude. Furthermore, pronuclear and antinuclear respondents have totally opposite perceptions as to whether nuclear power helps or hinders the attainment of these goals.

We found that the public is largely uninformed about nuclear power, and especially nuclear waste management. Most respondents greatly underestimate nuclear's role in electricity production, believe that most nuclear wastes are liquids stored in "Hanford-like" tanks, and overestimate the amount and longevity of nuclear wastes.

Environmentalists are more knowledgable about nuclear power than are nuclear neighbors and the general Washington public. Among the general public, however, those strongly supporting nuclear power possess significantly more nuclear knowledge than any of the other attitude groups. Also, on the three knowledge questions (all three related to waste management) that best predicted nuclear attitude, pronuclear respondents answered the questions correctly more often than antinuclear respondents.

Although human values and nuclear knowledge are strong determinants of one's nuclear power attitude, general energy beliefs and nuclear-specific beliefs add something more to the explanatory model. With regard to more general beliefs, pronuclear respondents believe that the United States economy will decline without increased energy production, whereas antinuclear respondents are not sure about the energy-economy relationship; antinuclear respondents believe that more conservation would make increased electrical production unnecessary, while pronuclear respondents believe that conservation alone won't be enough; and antinuclear respondents place more faith than pronuclear respondents in the ability of alternative energy technologies (especially solar power) to provide a large share of future energy needs. With regard to nuclear-specific attitudes we found that attitudes about nuclear safety, waste disposal, pollution, and reprocessing were most predictive of one's attitude about building more nuclear power plants.

Finally, our analysis of public policy issues has resulted in the issuance of the report entitled Public Policy Issues in Nuclear Waste Management. Four main clusters of issues surrounding waste management were identified and discussed: 1) temporal equity issues (fairness over time); 2) geographic and socioeconomic equity issues (fairness by region and social class); 3) implementation issues (organization, regulation, financial arrangements, and long-term management); and 4) public involvement issues (what can be gained or lost by public involvement, who should be involved, and conditions impeding or fostering public involvement). Of these issue areas, the temporal, geographic, and socioeconomic equity issues appear to be foremost in the present nuclear waste debate. A thorough analysis of how these issues impact waste disposal will also require that five related factors be taken into consideration: amount of waste, type of waste, type of waste disposal, irreversibility of disposal, and the inherent uncertainty in comparing the calculations of benefits and risks of different disposal modes over time.

PUBLIC PERCEPTION AND EVALUATION OF RISKS - M. K. Lindell and J. A. Hébert (HARC)

During the past quarter, work has been completed on the analysis of the risk tradeoffs questionnaire. A report on the survey's results, now completed and under review, describes the rationale and procedure for the sampling of intact groups and the formation of clusters of relatively homogeneous groups. This report's substantive focus is on those portions of the questionnaire most closely related to issues associated with nuclear disposal facilities. This includes questions about the perceived need for, and efficacy of, site control, site monitoring, and information transfer in producing system safety. Also included are the data on the minimum acceptable distance from technological facilities that respondents are willing to live or work.

Other data from this questionnaire will be presented in a subsequent report, now in the draft stage. This report will discuss systematic differences between pronuclear and antinuclear groups in the relative importance they attach to issues such as environmental pollution, energy shortage, and economic growth. The subsequent report will also show how these differences in issue salience are related to respondents' concerns about different aspects of energy technologies, especially risk.

A review draft of the questionnaire addressing the tradeoffs between public and occupational risk has been completed. Efforts are now under way to obtain commitments from groups to distribute this questionnaire to their members.

8.0 WASTE MANAGEMENT SAFETY STUDIES

W. K. Winegardner - Project Manager

Evaluate the safety of alternative waste management schemes for viable nuclear fuel cycles up to the final disposal step; develop the methodology necessary to permit the safety assessment; identify portions of waste management systems which could benefit by safety design emphasis.

SUMMARY

Once-through fuel cycle waste management operations were evaluated using safety indices based on such factors as radioactivity, volume, gamma power, heat generation, and radionuclide mobility and toxicity. Using assessment of ^{85}Kr management techniques, work continued on the development of insights concerning trade-offs between management by dispersion/dilution and by accumulation/containment. Seven different safety indices were examined to identify biases that could result from their application.

ONCE-THROUGH FUEL CYCLE ASSESSMENT - P. J. Pelto, J. W. Voss

The evaluation of the once-through fuel cycle waste management operations continued during the quarter. A specific reference system consisting of one pressurized water reactor and one 3000-MT away from reactor storage basin is being evaluated using the analysis methods outlined in earlier quarterly reports.(1,2)

The initial scoping analysis has been completed for the reference system and is shown in Tables 8.1 and 8.2. In this scoping analysis, safety indices based on such factors as radioactivity, volume, gamma power, heat generation, mobility, and toxicity are defined. These indices may be useful for providing relative comparisons of waste streams within a fuel cycle and of different fuel cycles.

The more detailed analysis of the reference system's waste streams is continuing. In this analysis, such factors as public safety, occupational safety, and cost will be quantified to the degree possible.

DISPERSION/ACCUMULATION TRADE-OFF ASSESSMENT - P. J. Mellinger

Work continued on methods for providing insights concerning trade-offs between management by dispersion/dilution and by accumulation/containment. Assessment of noble gas management techniques is being used as the basis for this work. An in-depth description of ^{85}Kr immobilization by high-temperature, high-pressure sorption on zeolite was completed. The use of high-pressure steel cylinders for ^{85}Kr storage was reviewed. Meteorological and population data were selected for use in siting a reference facility and calculating radiological consequence.

TABLE 8.1. Scoping Analysis Safety Indices of Reactor Wastes[a]

Waste Stream	Untreated Volume, m^3	Untreated Mass, kg	Activity, Ci	Toxicity Index m^3 air[b]	Gamma Power, MeV/sec[c]	Heat Generation, W	Mobility Index[d]	Available Technology Index[e]	Lifetime[f]
Trash	40	1.92×10^4	8	1.48×10^{10}	2.60×10^{11}	5.58×10^{-2}	4	1	25
Wet trash	550	1.65×10^6	5,880	1.07×10^{13}	1.74×10^{14}	3.71×10^{-1}	6	1	34
Noncombustible, noncompactable trash	40	4.0×10^4	16	2.13×10^{10}	5.55×10^{11}	1.22×10^{-1}	2	1	7.0
Core internals	5	2.5×10^3	156,000	1.85×10^{14}	5.52×10^{15}	1.22×10^{-3}	0	5	0.7

---

a. For annual reactor operations; treated wastes.
b. Air to dilute activity to recommended concentration guide.
c. Energy released in decay by gamma emission per unit time.
d. 0 = immobile, 10 = gaseous.
e. 0 = available technology, 10 = not available.
f. Percent of discharge radionuclides with half-life greater than 10 yr.

TABLE 8.2. Scoping Analysis Safety Indices for 3000-MTHM Away from Reactor Storage Basin[a]

Waste Stream	Treatment Options	Untreated Volume, m^3	Untreated Mass, kg	Activity, Ci	Toxicity Index m^3 air[c]	Gamma Power, MeV/sec[d]	Heat Generation, W	Mobility Index[e]	Available Technology Index[f]	Lifetime[g]
Spent fuel		NA	3.3×10^6	3.0×10^9	2.0×10^{21}	6.3×10^{19}	2.9×10^7	8	2	8.4
General trash	Compaction	92	4.5×10^4	9.0	1.3×10^{10}	1.9×10^{11}	3.8×10^{-2}	4	1	25
HEPA filters	Drumming	38	6.1×10^3	0.97	1.4×10^9	2.0×10^{10}	4.1×10^{-3}	4	1	25
Wet waste	Cementation	35	1.1×10^5	1.6×10^3	2.4×10^{12}	3.4×10^{13}	6.8	1	1	34
Noncombustible, noncompactable trash	Drumming	7	7.0×10^3	1.0	1.5×10^9	2.2×10^{10}	4.3×10^{-3}	2	1	7.5
Gaseous effluents	None									
^3H		NA	2.5×10^{4}[b]	1.2	6.0×10^6	NA	1.3×10^{-4}	10	1	100
^{85}Kr		NA	6.5×10^{-4}	2.1×10^2	7.0×10^8	NA	8.2×10^{-1}	10	1	100
^{129}I		NA	4.7×10^{-3}	1.7×10^{-4}	8.5×10^6	NA	1.9×10^{-7}	10	1	100

---

a. For treated wastes; annual quantities for receiving 410 MTHM and storing 2460 MTHM.
b. Mass of excess water vaporized annually.
c. Air to dilute activity to recommended concentration guide.
d. Energy released in decay by gamma emission per unit time.
e. 0 = immobile, 10 = gaseous.
f. 0 = available technology, 10 = not available.
g. Percent of discharge radionuclides with half-life greater than 10 yr.

USE OF INDICES - J. W. Voss

Seven different safety indices, defined in Table 8.3, were examined to identify biases which could result from their respective application. The use of safety indices in waste management safety studies is one alternative assessment technique. In particular applications, if their limitations are understood, safety indices can provide valuable insights into safety. However, use of safety indices should be avoided unless it is fully understood that they do not account for waste form characteristics, facility designs, or environmental behavior.

The seven indices have been examined on the basis of their prediction of the time-dependent hazard of the packaged spent fuel from the once-through fuel cycle. The safety indices normalized to unity at time zero are plotted as functions of time in Figure 8.1. The HM1, HM2, PHM and RTI are calculated on the basis of airborne release, while HM and HI assume a water release. Figure 8.1 reveals that after 10^6 years of decay, the normalized indices vary

TABLE 8.3. Safety Indices

Index Title	Definition	Reference
Total Radioactivity[a]	$Q = \sum_{i=1}^{n} Qi(t)$	Bell(3)
Hazard Measure[b]	$HM = \sum_{i=1}^{n} \frac{Qi(t)}{RCGi}$	Bell(3) and USNRC(4)
Modified Hazard Measure 1(c)	$HM1 = \sum_{i=1}^{n} Qi(t)[(ai/MPlwi) + (bi/MPlai)]$	McGrath(5)
Modified Hazard Measure 2(d)	$HM2 = \sum_{i=1}^{n} \int_{t}^{t+di} [Qi(t')/MPli]dt'$	Smith and Kastenberg(6)
Potential Hazard Measure(e)	$PHM = \sum_{i=1}^{n} \left\{[PiQi(t)]/[MPli\ \lambda_i]\right\}$	Gera and Jacobs(7)
Hazard Index(f)	$HI = \sum_{i=1}^{n} \frac{Qi(t)/V}{RCGi}$	Claiborne(8)
Relative Toxicity Index	$RTI = \frac{\left(\sum_{i-1}^{n} HMi\right)_{Waste}}{\left(\sum_{j=1}^{n} HMj\right)_{Baseline}}$	Hamstra(9)

---

a. Qi(t) = Total radioactivity of isotope i as a function of time.

b. RCGwi, RCGai = Recommended concentration guide of isotope i in water or air, respectively.

c. ai, bi = Fraction of isotope i released to water or air, respectively. MPlwi, MPlai = Maximum permissible intake of isotope i in water or air, respectively.

d. di = Time period of concern for the release of isotope i to the environment.

e. Pi = Probability of release of isotope i to the environment; λ_i = specific radioactivity of isotope i.

f. V = Volume in which the waste is contained.

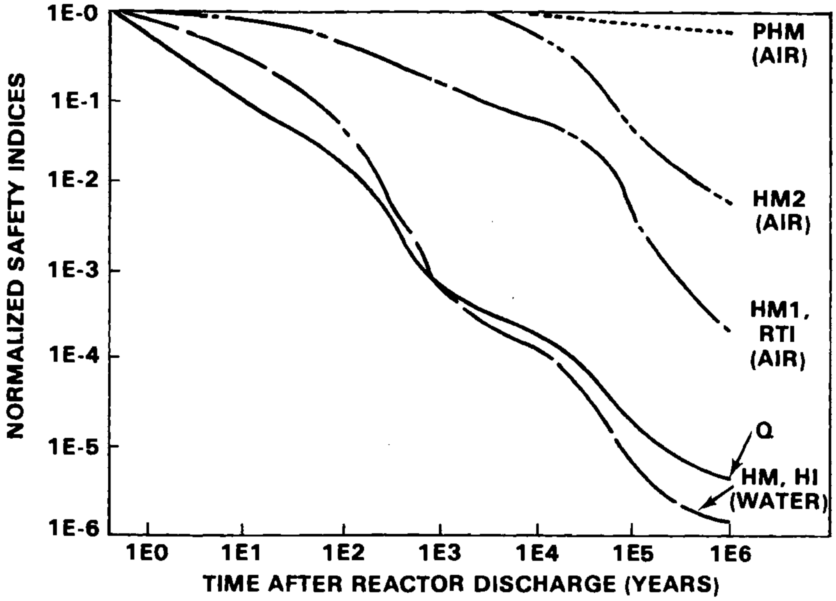

FIGURE 8.1. Normalized Safety Indices for Packaged Spent Fuel from the Once-Through Fuel Cycle

by nearly six orders of magnitude.

On the basis of the PHM plot (in air), one could conclude that the hazard associated with spent fuel decreases less than a factor of two with 10^6 years of decay. However, the value of PHM is numerically dominated by the presence of ^{238}U, which accounts for 95% of the total. By application of the HM2 (in air), one could conclude that the hazard of spent fuel does not decrease over periods less than 5000 years. Numerically this results from the presence of ^{239}Pu and ^{240}Pu. Both effects result from the fact that PHM and HM2 are directly proportional to the half-lives of the isotopes being considered. Further, the presence of α-emitters in the waste system is numerically amplified because both indices are inversely proportional to RCG values which in air may be several orders of magnitude lower for α-emitters than for β- or γ-emitters. The application of HM1 and RTI (in air) may lead to the conclusion that the hazards associated with spent fuel decrease significantly for decay periods greater than 5000 years. Again, this conclusion is the result of ^{239}Pu and ^{240}Pu decay. Unlike the PHM and HM2 plots, the HM1 and RTI do reflect the decay of short-lived radionuclides. This results because the PHM and HM2 are directly proportional to the half-life of the constituents, whereas HM1 and RTI are not. Examination of the normalized plots of HM and HI reveals the prediction that the hazard associated with spent fuel in water is similar to the total radioactivity over time, and that the hazard drops nearly six orders of magnitude over 10^6 years of decay.

In summary, the safety indices calculated for airborne releases are numerically dominated by the presence of α-emitters, without regard to their actual toxicity in specific scenarios. Safety indices calculated for water releases roughly assign equal hazard to all radionuclides because the RCG values are relatively invariant for the isotopes found in spent fuel. However, the behavior of these radionuclides in the environment is not reflected, so that the very mobile isotopes are indistinguishable from the relatively immobile. The safety indices proportional to the half-lives of the radionuclides may be numerically dominated by isotopes in either extreme (depending on the form). The total radioactivity as a safety index does not reflect any information about the toxicity or environmental behavior of the radionuclides being considered.

REFERENCES

1. A. M. Platt, compiler, Nuclear Waste Management Quarterly Progress Report, January through March 1978. PNL-2378-1, Battelle, Pacific Northwest Laboratories, Richland, WA.
2. A. M. Platt, compiler, Nuclear Waste Management Quarterly Progress Report, April through June 1978. PNL-2378-2, Battelle, Pacific Northwest Laboratories, Richland, WA.
3. M. J. Bell, ORIGEN - The ORNL Isotope Generation and Depletion Code, ORNL-4258, Oak Ridge National Laboratory, Oak Ridge, TN, May 1973.
4. USNRC, Code of Federal Regulations, Title 10, Chapter 1, Part 20, 1976.
5. P. E. McGrath, Radioactive Waste Management Potentials and Hazards from a Risk Point of View, KFK-1972, 1974.
6. C. F. Smith and W. E. Kastenberg, Nuclear Engineering Des., 39:293-333, 1974.
7. F. Gera and D. G. Jacobs, Considerations in Long-Term Management of High-Level Radioactive Wastes. ORNL-4762, Oak Ridge National Laboratory, Oak Ridge, TN, February 1972.
8. H. C. Claiborne, Effect of Actinide Removal on the Long-Term Hazard of High-Level Waste, ORNL-TM-4724, Oak Ridge National Laboratory, Oak Ridge, TN, January 1975.
9. J. Hamstra, Nuclear Safety, 16:2, 1975.

9.0 WASTE ISOLATION SAFETY ASSESSMENT PROGRAM

Albin Brandstetter - Project Manager
Mark A. Harwell - Assistant Project Manager

The objectives of the Waste Isolation Safety Assessment Program (WISAP) are to:

1. *develop the generic methods needed to assess the long-term safety of geologic isolation repositories*
2. *obtain the generic and site-specific data necessary to apply the methods*
3. *demonstrate the use of the methods for a specific site*
4. *apply the methods to make safety assessments for sites of the National Waste Terminal Storage Program*
5. *analyze societal acceptance issues and develop methods of communicating assessment results which enhance the rational resolution of those issues.*

SUMMARY

During this quarter a management task was established, including assignment of a new project manager and assistant project manager and support staff. There was also a substantial replacement of the Task 1 personnel. External control shifted from the Office of Waste Isolation (OWI) to the Office of Nuclear Waste Isolation (ONWI). With these changes, the scope and direction of WISAP were reviewed and new emphasis was added to more timely production of safety assessments focused on the anticipated licensing requirements. Examples are the exercising of the WISAP geosphere and dose models for an initial assessment of the Paradox Basin bedded salt site, and the establishing of the framework within the scenario analysis task for expert-opinion input to the consequence analysis task.

Additional efforts during this quarter included progress on a number of reports or drafts, the development of the release scenario pilot program to an operational level, the continued development of sorption- and leach-testing facilities and data, and continued transport and dose model development or conversions. An overview of WISAP was presented at the Meeting on Radionuclide Migration in Crystalline Rocks held by the Nuclear Energy Agency at Studsvik, Sweden (PNL-SA-7184).

TASK 1 - RELEASE SCENARIO ANALYSIS - R. A. Craig and G. L. Benson

This quarter was largely one of transition to new staff, review of the scope and emphasis of the task efforts, planning for the shift to more timely production of release scenarios and establishing the framework for expert-opinion, geology-specific scenario analyses. The pilot program for prediction of geologic scenario probabilities has been completed, programmed, and debugged. Exercise of this program was begun and will continue, to aid in developing a more realistic scenario analysis program. The theoretical framework of this simulation modeling has been outlined.

Most of the geologic consultants have submitted their final reports with precis, which will be integrated into a summary document. The FY-1977 Task Workshop report has been prepared and submitted for clearance. Planning efforts have included identifying the expert-opinion teams that will provide scenarios for the geosphere transport site analyses during FY-1979 and will provide input to the model development.

TASK 2 - WASTE FORM RELEASE RATE DATA - D. J. Bradley and R. P. Turcotte

The metallographic studies of spent fuel were completed. Leaching and analysis work continued on spent fuel and actinide-doped glass, using simulated ground waters and salt brine solutions. Building modifications to accommodate a glovebox and open-face hood were completed, and this unit installation is 90% complete. Further leaching tests have been planned to use this equipment, including static leach tests on actinides. Fabrication of a large hot cell leach testing cabinet has been completed, and preparations are under way for installation in the hot cell. This unit will accommodate up to 150 leach tests simultaneously. The autoclaves for nonradioactive and doped waste form studies have been received and installed. Additionally, a system of three autoclaves for hot cell use has been designed and put out for bid.

Leaching and analysis work continued at Lawrence Livermore Laboratories (LLL) using the single-pass leaching system. A paper co-authored with PNL for presentation at the Materials Research Society meeting in November has been accepted.

The compositions of four transuranic (TRU) waste forms have been developed at Brookhaven National Laboratory (BNL). Procurement of actual incinerator ash from Rocky Flats is in progress. Upon receipt of this ash, the TRU waste forms will be made and leach tests started using the same leaching solutions as at PNL and Lawrence Livermore Laboratory. Construction of a semi-automated leaching system for this study is 75% complete.

TASK 3 - RELEASE CONSEQUENCE ANALYSIS - J. R. Raymond

In response to the WISAP Review Committee, during this quarter an initial site-specific exercise of the consequence analysis models was performed. This involved a cooperative effort for the Paradox Basin site in Utah with Bechtel National, Inc., in developing the data base, conceptual and numerical models, and release scenario for analysis by Task 3. The VTT ground-water code was used for hydrologic modeling, and a one-dimensional MMT code was used for radionuclide transport simulation.

This exercise was completed for a single set of parameters and initial conditions and reported to the WISAP Review Committee.

The 1978 Task 3 Workshop was held at PNL, with presentations on each of the geosphere models for peer review of the WISAP approach to consequence analyses. Verification and sensitivity analysis of the 3-D finite element (FE) ground-water flow model with the PATHS analytical solution was completed and included in the draft document on the FE model. The FE solution was compared to the analytical Theis nonequilibrium equation for a single aquifer system. Data base programs were developed to display and plot stratigraphic sections and to project sections onto defined reference lines. The PATHS documentation was issued (BCSR-38) and the FY-1977 workshop report cleared (PNL-SA-7468). Conversion of computer codes required for dose calculations was nearly completed this quarter. ARRRG, FOOD, DACRIN, KRONIC, and SUBDOSA are fully operational; SUBDOPA is 80% debugged, PABLM, a newer version of FOOD, is being converted.

TASK 4 - TRANSPORT DATA - R. J. Serne

The studies at PNL and several subcontractors to resolve method-dependent sorption/desorption discrepancies have continued during this quarter, including batch K_d method comparisons with axial filtration, channel chromatography, and flow-through column systems. To date, results show that favorable comparisons can be obtained with careful experimentation for selected media/solution systems. Tests using more nuclide/rock/ground-water combinations continue. A preliminary experiment using a tuff core was begun for comparison of migration rates through intact rock versus disaggregated rocks.

The data collection efforts continued at PNL and the subcontractors for expanding the defensible data base of sorption of various nuclides by a wide range of representative geologic media and ground-water types. Data were collected this quarter for K_d values for I, Tc, Np, Pu, Am, Sr, Cs, Eu, and Ce onto media such as shale, granite, limestone, basalt, tuff, and numerous pure minerals, using synthetic salt brines and ground waters. These data, and others from the literature, are being processed by Adaptronics using adaptive learning networks to produce multinomial equations relating K_d values for a radionuclide to characteristics of the media and methodology used. Thermodynamic data on solid compounds and solution species of many different radionuclides were published (PNL-2651).

Basic research into the factors and interactions controlling sorption/desorption of radionuclides included studies on the effect of ionic strength and tracer concentration.

Other studies focused on the redox potential threshold for creation of insoluble compounds (at Oak Ridge National Laboratory), microautoradiography of nuclide/rock matrix interfaces (at Los Alamos Scientific Laboratories and Lawrence Berkeley Laboratory), adsorption kinetics (at Argonne National Laboratory and Rockwell Hanford Operations), ground-water valence states (at PNL), and potential for migration of radionuclides through geologic media as polymeric-colloidal species (at Georgia Institute of Technology).

The report for the 1977 Workshop was published this quarter (PNL-SA-6957), and preparations were made for each subcontractor to present FY-1978 progress reports at the 1978 workshop to be held October 2-5, 1978. Several abstracts were also prepared by subcontractors for waste management conferences of the American Chemical Society, Materials Research Society, and the Organization for Economic Cooperation and Development (OECD).

TASK 5 - SOCIETAL ACCEPTANCE - A. H. Schilling

During this quarter, Activity at the Human Affairs Research Center (HARC) for Task 5 focused on completion of the writing and reviewing of the final three reports of this task, upon ending this quarter, Task 5 activities as a part of the WISAP are terminated.

REPORTS ISSUED DURING QUARTER

D. H. Rai and R. J. Serne, Solid Phases and Solution Species of Different Elements in Geologic Environments. PNL-2651, Pacific Northwest Laboratory.

R. J. Serne, Ed., Waste Isolation Safety Assessment Program. Task 4. Contractor Information Meeting Proceedings. September 21-23, 1977. PNL-SA-6957, Pacific Northwest Laboratory.

R. W. Nelson and J. A. Schur, A Preliminary Evaluation Capability for Some Two-Dimensional Groundwater Contamination Problems. BCSR-38, BCS Richland, Inc.

R. J. Cole, K. V. Friedman, F. A. Morris, and S. Smolkin, Compensation for the Adverse Effect of Nuclear Waste Facilities.

R. F. Smith, State and Local Regulations Relevant to Nuclear Waste Isolation Facilities.

T. Hunter, Nuclear Waste Repository Land Use Control Considerations in Selected States.

10.0 WELL LOGGING INSTRUMENTATION DEVELOPMENT FOR SHALLOW LAND BURIAL

R. L. Brodzinski - Project Manager

The objectives of this research program are to develop appropriate well-logging equipment capable of determining ^{90}Sr*,* ^{3}H*, and the transuranics at sensitivity levels which will provide useful information for the proper operation of a land burial site.*

SUMMARY

A viable technique for the determination of ^{90}Sr by well-logging measurement of bremsstrahlung radiation is described. Detection limits are given for determination of ^{90}Sr as a function of counting time and the concentration of interfering gamma-ray-emitting radionuclides. Experiments have been completed to determine the optimum detector configuration for this technique.

The use of ultrathin plastic scintillators for the direct well-logging determination of tritium in water is being investigated.

Passive neutron detection techniques for quantitative analysis of plutonium, americium, and curium isotopes in soil are being calibrated as a function of soil moisture. Experiments are in progress to determine the sensitivity and detection limits for measuring these actinides by photon well-logging.

DEVELOPMENT OF LOGGING SYSTEMS CAPABLE OF MEASURING ^{90}Sr - R. L. Brodzinski and H. L. Nielson

The bremsstrahlung radiation generated by the deceleration of ^{90}Sr(^{90}Y) beta particles can be detected with a germanium diode spectrometer and used to quantitatively determine ^{90}Sr concentrations. This bremsstrahlung contribution can be resolved even in the presence of interfering gamma-ray-emitting radionuclides. Figure 10.1 depicts a ^{90}Sr(^{90}Y) bremsstrahlung spectrum superimposed on a typical fission product gamma-ray spectrum as measured from a well in homogeneously contaminated soil. The major portion of the bremsstrahlung activity falls between 60 and 236 keV. Fortunately, this energy range does not contain resolvable fission product photopeaks in any of the systems studied thus far.(1) Compton scattered photons are observed in this area; however, their contribution to the total number of integrated events can be corrected for by quantative measurement of the concentrations of the various radionuclides that produce these interfering gamma-rays. Since these concentrations can be determined by measuring appropriate photopeaks,(1) the number of scattered events in the 60-236 keV range can be determined by measurement of these full-energy peaks. Subtraction of this Compton component and the background from the integrated area leaves the net contribution from

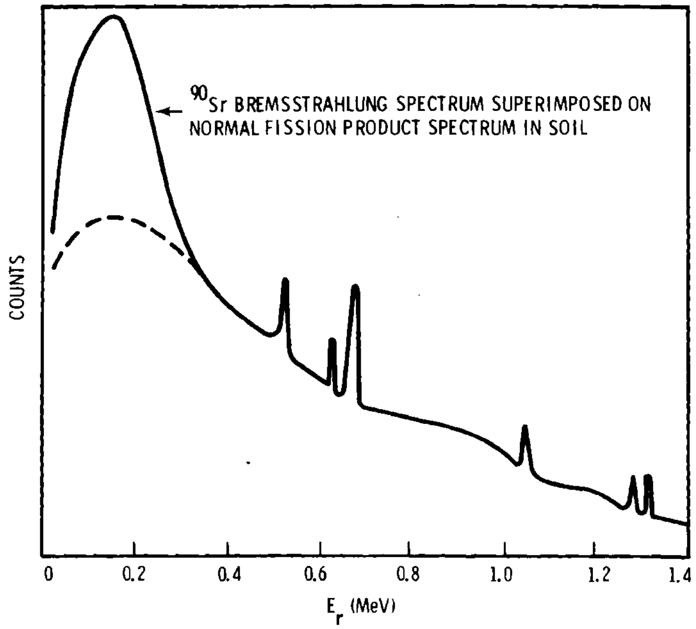

7814419-2

FIGURE 10.1. Components of Gamma-Ray Spectrum from Fission Products in Soil

^{90}Sr(^{90}Y). Appropriate calibration leads to quantitative ^{90}Sr concentration values.

The sensitivity of this well-logging technique for the determination of ^{90}Sr in typical fission product activities was obtained using point sources of various radionuclides in a calibration facility filled with Hanford sediments. Data representing homogeneous distribution of the activities in an infinite volume of soil are obtained by normalizing each calibration measurement to unit concentration of radioactivity in concentric spherical shells and summing over all significant shells. The details of this calibration technique and verification of its accuracy have been given elsewhere(1,2) and will not be repeated here. Data were obtained separately and in combination using a 3.482 mCi ^{90}Sr source and a mixed fission source containing: 582.2 μCi ^{137}Cs; 89.88 μCi ^{106}Ru; 27.86 μCi ^{144}Ce; 7.252 μCi ^{134}Cs; 4.543 μCi ^{125}Sb; and 1.167 μCi ^{154}Eu.

To avoid unnecessary expense, an approximation was utilized in this demonstration proof-of-concept experiment. The fraction of Compton scattered events in the 60-236 keV range was not determined separately for each gamma-ray-emitting fission product, but was determined for the "typical" mixture of fission products described earlier. In this case, the fraction of Compton events was not measured relative to any particular photopeak(s), but was measured relative to the scattered events in the energy range 238-400 keV--an area also devoid of photopeaks from these radioisotopes. Simultaneous equations and the spectral shape difference between Compton scattered photons and bremsstrahlung radiation are used to determine net ^{90}Sr contributions from a mixture of ^{90}Sr and gamma-ray-emitting radionuclides. The energy range 60-236 keV is called area No. 1, and the energy range 238-400 keV is area No. 2. These areas are identified as subscripts in the following equations. Similarly, the letter B will denote the bremsstrahlung contribution in an area, and the letter C will be used for the Compton contribution. The net normalized values of B_1, B_2, C_1, and C_2 are determined for a given detector system as described earlier. The spectral shape difference is always such that $B_1/B_2 > C_1/C_2$. To determine the ^{90}Sr contribution from a measurement of a mixture of ^{90}Sr and gamma-ray emitters, let x denote the net counts in area No. 1 and y denote the net counts in area No. 2. Then

$$B_1 + C_1 = x \qquad (1)$$

and

$$B_2 + C_2 = y. \qquad (2)$$

From calibrations and definition

$$B_1/B_2 \equiv \alpha \qquad (3)$$

and

$$C_1/C_2 \equiv \beta \qquad (4)$$

Solving for the ^{90}Sr contribution,

$$B_1 = \frac{\alpha\ (x-\beta y)}{\alpha-\beta} \qquad (5)$$

The validity of Equation 5 was demonstrated experimentally by counting known quantities of ^{90}Sr in gamma-emitting fission products.

In actual practice, these calculations would be done on-line in real time, and the Compton contribution to area No. 1 would be calculated and subtracted for each individual radionuclide contributing to the spectrum based on calibrations with isotopically pure sources. In this operational system, the correction would be determined by integration of approipriate full energy photopeaks with automatic data processing equipment. These calibrations also correct for the bremsstrahlung contribution from isotopes other than $^{90}Sr(^{90}Y)$.

Due to individual detector response characteristics, it will be necessary to calibrate each field instrument separately. Since the detectors used in these experiments are not likely to be used as field instruments, and since appropriate ADP equipment was not available, the approximation technique was used to demonstrate proof-of-concept and to obtain sensitivities and detection limits in the most economical manner possible. If this logging technique proves to be the optimum method for determining ^{90}Sr in a shallow-land burial ground, the field detector to be used will be calibrated with individual radioisotopic sources, and the Compton correction factors will be based on full-energy photopeaks.

Two sizes of intrinsic germanium diodes were used in these experiments to determine which would be more sensitive for measuring ^{90}Sr in a gamma-ray field. One detector had an active volume of 0.5 cm^3, and the other was 102 cm^3. In theory, the larger diode could be expected to be more sensitive due to its higher efficiency. However, the smaller diode might be expected to be more sensitive since its efficiency loss is greatest in the gamma-ray energy range and only minimal in the bremsstrahlung energy range.

This results in an increase in the signal-to-noise ratio and could lead to enhanced sensitivity. Figures 10.2 and 10.3, detection limit curves for these diodes as a function of counting period and gamma-ray concentration, show graphically that the larger diode demonstrated greater sensitivity by about a factor of four under all test conditions. These detection limits were calculated by setting the ^{90}Sr bremsstrahlung activity, B_1 in Equation 5, equal to the statistical uncertainty of all factors in the right-hand side of that equation. As can be seen in Figure 10.3, a ^{90}Sr concentration of less than 10 nCi cm^{-3} can be detected in a fission product gamma field of 100 nCi cm^{-3} in a counting period of only 10 sec. Similarly, in a relatively gamma-free environment, a ^{90}Sr concentration of <0.01 nCi cm^{-3} can be measured in less than 3 hr.

A paper entitled "A Well Logging Technique for the In Situ Determination of ^{90}Sr" by R. L. Brodzinski and H. L. Nielson, based on these experiments, has been submitted for publication in the Proceedings of a Symposium on Recent Advances in Nuclear Analytical Methods to be held April 1-6, 1979, in Honolulu.

A large-volume intrinsic germanium diode has been acquired which is designed specifically for well logging applications and capable of use in wells as small as 3 in. in diameter. This detector is operable in any orientation throughout 4π and is designed for attachment of a neutron source for in situ activation analysis.

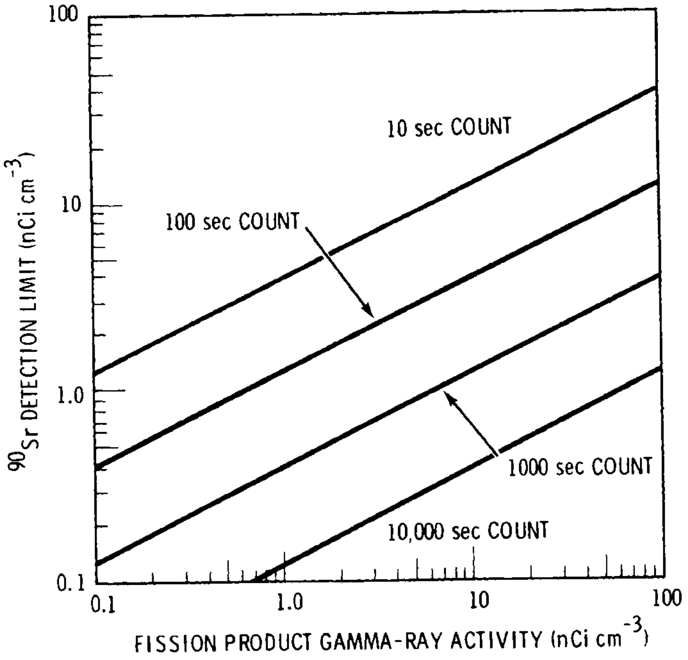

7900024-1

FIGURE 10.2. Bremsstrahlung Detection Limits for ^{90}Sr in Soil Contaminated with Gamma-Ray-Emitting Fission Products Using a 0.5 cm^3 Intrinsic Germanium Diode

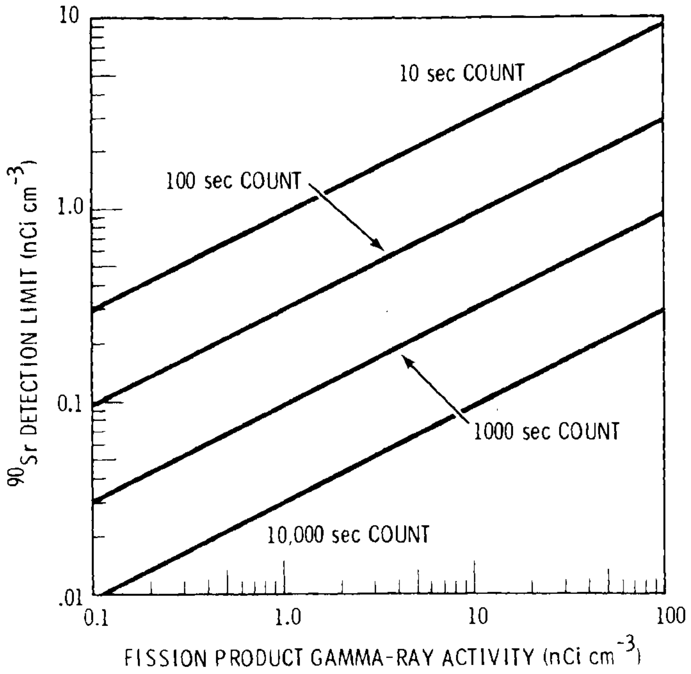

7814419-1

FIGURE 10.3. Bremsstrahlung Detection Limits for ^{90}Sr in Soil Contaminated with Gamma-Ray-Emitting Fission Products Using a 102 cm^3 Intrinsic Germanium Diode

Although this detector was obtained with other program funding, it will be made available for testing and use in this program.

DEVELOPMENT OF LOGGING SYSTEMS CAPABLE OF MEASURING TRITIUM - A. C. Case and R. L. Brodzinski

The direct well logging measurement of tritium in water utilizing ultrathin plastic scintillators is being considered. Methods are being examined for applying this technique to the analysis of gaseous as well as aqueous tritium, for increasing the sensitivity, and for reducing potential interferences.

DEVELOPMENT OF LOGGING SYSTEMS CAPABLE OF MEASURING ACTINIDES - R. L. Brodzinski

Calibration of the passive neutron detection technique has been initiated at a soil moisture level of 16%. A paper entitled "A Technique for the In Situ Determination of Transuranic Elements in Relatively Inaccessible Locations" by R. L. Brodzinski, which is based on this research, has been submitted for publication in the *Proceedings of a Symposium on Recent Advances in Nuclear Analytical Methods*, to be held April 1-6, 1979, in Honolulu. Another paper entitled "A Technique for In Situ Moisture Level Determinations in Relatively Inaccessible

Matrices" by R. L. Brodzinski, which is a by-product of this research, has also been submitted for the same symposium.

Experiments are in progress to determine the sensitivity and detection limits for measuring actinides by photon well logging. The procedures are similar to the ^{90}Sr bremsstrahlung experiments, and optimum photopeak energies, diode configuration, and interference rejection parameters are being determined. Measurements have been made on ^{241}Am, ^{243}Am, ^{244}Cm, and several Pu isotopes. The large-volume germanium well logging detector described above should also prove useful in this portion of the research.

REFERENCES

1. H. L. Nielson, N. A. Wogman, and R. L. Brodzinski, "In Situ Subterranean Gamma-Ray Spectroscopy," Nuclear Instrm. Methods, 143:385, 1977.
2. R. L. Brodzinski and N. A. Wogman, "In Situ Quantitative Determination of Transuranic Elements in Areas of High-Level Gamma Radiation," NBS Special Publication 528, Analytical Methods for Safeguards and Accountability Measurements of Special Nuclear Materials, p. 253, 1978.

11.0 MONITORING AND PHYSICAL CHARACTERIZATION OF UNSATURATED ZONE TRANSPORT

S. J. Phillips - Project Manager

The objective of this project is to develop monitoring instrumentation systems and burial media-waste characterization methods to evaluate the migration of contaminants from disposal sites for low-level solid waste.

SUMMARY

Transport of radionuclides in unsaturated sediments was measured in test columns in the laboratory. ^{60}Co-EDTA complex and ^{95m}Tc were tested at soil water contents less than 50% saturation. Effluent breakthrough curves were analyzed to determine the retardation factors and distribution coefficients for these isotopes. The breakthrough curves of ^{95m}Tc were similar to those of chloride at similar water contents. ^{60}Co-EDTA breakthrough was retarded with respect to ^{95m}Tc. Batch Kd values for ^{60}Co-EDTA and ^{95m}Tc generally agreed with column Kd values, but the column Kd values could be determined with greater precision than batch Kd values.

Field studies continued. Monitoring of water transport by neutron probe and weighing lysimeter were evaluated. Comparison over a 35-day period demonstrated agreement between methods to within ±0.2 cm (water depth equivalents). Suitable agreement between methods requires field calibration of the neutron probe and accounting for mass transport of sediment from the weighing lysimeter.*

LABORATORY ANALYSIS - G. W. Gee and A. C. Campbell

Unsaturated column tests were continued. The experimental arrangement for producing steady flow in unsaturated columns was detailed in a previous report.(1) The columns were leached with a low-salt solution [0.15 $\underline{M}$ $NaNO_3$, 0.01 $\underline{M}$ KNO_3, and 0.002 $\underline{M}$ $Ca(NO_3)_2$] at a flow rate of 6.4 cm/day while the lower boundary of the columns were controlled at a 43-cm H_2O tension by a regulated vacuum control. Tracer pulses of ^{95m}Tc and ^{60}Co-EDTA were applied to the unsaturated column. Table 11.1 shows the results of two tracer flow tests on soil B, a sandy soil representative of surface soil materials found near the 300 North Burial grounds about 2 km southeast of the Fast Flux Test Facility on the Hanford Reservation. (See previous reports for physical characterization of soil B.)

---

* See PNL-2377-4 for background material related to this program.

TABLE 11.1. Calculated and Measured Breakthrough Curve Parameters for ^{95m}Tc and ^{60}Co-EDTA in Soil B

Isotope	Pulse Period,[a] days	Pulse Volume Ratio Computed	Pulse Volume Ratio Measured	R Factor	Kd Column	Kd Batch
^{95m}Tc	1.33	1.87	1.88	1.01	+0.001	-2.98 ± 2
	2.17	2.87	2.86	0.97	-0.003	
^{60}Co-EDTA	1.33	1.87	1.88	1.39	0.039	0.06 ± 1.0
	2.17	2.86	2.86	1.34	0.034	

---

a. Flow velocity was 6.4 cm/day at 43% saturation.

Kd values were calculated using the equation

$$Kd = (R-1)\,\frac{\theta}{\rho}$$

where

R = retardation factor

θ = volumetric water content (cm^3/cm^3)

ρ = soil bulk density (g/cm^3).

The computed pulse volume ratios and retardation factors in Table 11.1 were determined from a curve-fitting routine (Wierenga, 1978, personal communication) which best fit the effluent data to the normal convective-dispersive equation. The computed and the measured pore volumes are in excellent agreement. The Kd (distribution coefficient) values from the columns are in reasonable agreement with each other for the two pulse periods for each of the tested isotopes. The mean Kd values were -0.001 and +0.037 for technetium and cobalt, respectively. A slightly negative Kd value for technetium is not surprising since technetium was in a negative one valence state throughout the test and hence was excluded from the exchange sites of the clay present in the B soil. The cobalt complex, on the other hand, was slightly retarded, and the low but positive Kd value of cobalt correlated well with the observed retardation.

The batch Kd values (determined in the conventional manner and reported in Table 11.1) for cobalt show good agreement with the column Kd values but suggest an even greater anion exclusion than was observed. Anion exclusion in soil B appears to be present, as indicated by both column and batch Kd evaluations. From additional testing it was observed that the pore volumes of effluent producing a relative concentration of 0.5 were 0.74 ± 0.07, 0.90 ± 0.03 and 1.19 ± 0.04 for chloride, technetium, and cobalt-EDTA, respectively. Since breakthrough occurs prior to one pore volume for both chloride and technetium, it may lend further support to anion exclusion since chloride is also known to be excluded from clay exchange sites. However, the breakthrough prior to one pore volume at 0.5 relative concentration can also be explained by the relative fraction of mobile water present. Gaudet et al. (1977)[2] have shown that as the fraction of mobile water decreases the chloride breakthrough occurs at an increasingly earlier time because of water trapped in dead end pores. Additional testing with a noninteracting isotope such as tritium and additional tests at lower water contents should aid in assessing both the contribution of anion exclusion and the effects of "dead end" porosity in causing the early breakthrough observed in these unsaturated columns.

FIELD MONITORING AND DATA EVALUATION - M. D. Campbell, K. O. Schwarzmiller, and G. W. Gee

Measurements were continued at the field test site. Temperatures of air and soil profiles have been monitored at 2-hr intervals since July 14, 1978. Fiberglass resistance blocks and soil psychrometers with temperature thermocouples were fastened to a positioning frame and placed in the soil at the 2.5, 5, 10, 15, and 30-cm depth below the ring-leveled soil surface in the north and south caissons. These were connected to a Wescor Data Logger and monitored at 2-hr intervals.

Lack of AC power at the site required special DC power arrangements. A 200-amp-hr, 12-volt battery was placed in the instrument caisson; and a remote switch, triggered by the data logger when it turns on to scan, was installed to turn on an inverter which provides 120 volts AC power necessary to operate the weighing lysimeter readout system. This installation was completed August 14, 1978. Thereafter weight data were logged on 2-hr intervals, using a bucking voltage on the Weightronix (lysimeter) analog output to bring it in range for the Wescot Data Logger. A combination power plant-welder and some small battery chargers were purchased to recharge the battery. After some difficulty from leaving the power plant turned on, an automatic shutoff system was designed and installed to turn the power plant off when the battery was fully recharged.

During mid-August, an infrared optical thermometer was borrowed for monitoring surface temperature to be compared with the in situ thermocouple temperature values monitored by the data logger. Although good data were collected on August 15 and 16, 1978, the rapidly changing weather has since prevented our obtaining measurements of maximum surface temperature and detailed near-surface temperature profiles. The in situ temperature profiles look good; however, the surface temperature has to be inferred.

Additional thermocouple psychrometers, resistance-type moisture blocks, and heat dissipation units were installed in the two large caissons, but modification of the heat dissipation units has proven necessary to maintain proper hydraulic contact with the soil. The thermocouple psychrometers have not yielded useful moisture data because the sensors cannot detect water content or potential changes when the water potential is in the range from 0 to -1 bars. At lower water potentials, which occur near the soil surface, the sensors show effects of thermal loads, and outputs are erratic. On the other hand, resistance blocks were observed to be sensitive to transient moisture changes, particularly when the soil is wet. Data evaluation of the observed moisture changes has begun.

Neutron probe moisture data have been collected and compared with lysimeter data, with agreement between results to within about 0.2 cm of water over the test interval (35-day period). The test period was from August 18 to September 22 (Julian dates 230 to 265). During this period, there was only one major precipitation event, when 1.5 cm of rain was recorded on day 234. Four other days had measurable precipitation, but none of these events exceeded 0.2 cm. Measurement comparisons were made six times during the period. The data were matched on August 18. On day 237, 4 days after the 1.5-cm rainstorm, the neutron probe underestimated storage by 0.20 cm. On day 265, at the end of the test period, the neutron probe overestimated storage by 0.25 cm. At all other measurement periods, measurements of water storage by neutron probe and by lysimeter agreed to within 0.2 cm. The difference in water storage inferred from lysimeter and neutron probe measurements at the end of the test period was probably caused by observed soil losses from the lysimeter as a result of wind transport. Although a correction was made for estimated losses (15 kg), the actual loss may have been 15 kg larger, which would account for the observed difference. The bare exposed lysimeter surface requires careful maintenance to insure at least ±0.2 cm precision in the water storage measurements. This will require maintaining the total soil weight to within ±5 kg.

REFERENCES

1. A. M. Platt, compiler, Nuclear Waste Management Quarterly Progress Report April Through June 1978. PNL-2378-2, Pacific Northwest Laboratory, Richland, WA, November 1978.

2. J. P. Gaudet, H. Jegat, G. Vachaud, and P. J. Wierenga, "Solute Transfer, with Exchange Between Mobile and Stagnant Water, Through Unsaturated Sand." Soil Sci. Soc. Am. J., 41:665-670, 1977.

12.0 DETECTION AND CHARACTERIZATION OF MOBILE ORGANIC COMPLEXES OF FISSION PROJECTS

J. A. Franz - Project Manager

The objective of this project is to determine the important mobile or volatile nontransuranic organic complexes of fission and activation products found in the storage of low-level waste in shallow-land burial facilities and to determine the role of organic complexing agents in enhancing the mobility of nuclides in soil.

SUMMARY

Detection of ^{93}Nb and ^{91}Zr nuclear magnetic resonance (NMR) transitions was attempted without success, apparently due to very short T_1 relaxation times dominated by quadrupole relaxation. Previous studies of tartrate and gluconate complexes of zirconium were expanded to include EDTA and DTPA complexes because these complexes were found to exhibit up to 10^{-4} M aqueous solubility. The study of these complexes completes all planned work with zirconium complexes. Procedures were identified for detecting citrate eluent in the ion exchange separation of technetium complexes. Due to the close relationship between nickel and cobalt complexes, the proposed work with nickel complexes was deferred in favor of the less well characterized complexes of technetium. Combined NMR/liquid chromatography techniques were developed for monitoring the purification of technetium complexes.

IDENTIFICATION OF NUCLIDES AND COMPLEXING AGENTS - J. A. Franz

This task involves the continual refinement of our existing data on complexes and nuclides. Recently available data(1,2) dealing with waste inventories of Maxey Flats and Oak Ridge National Laboratory do not include estimates of low-level nontransuranics ^{93}Zr and ^{95}Zr. Thus, while it is clear from inventories that the major fission products such as ^{10}Co, ^{239}Pu, *et al.* exist in substantial quantities and are subject to organic-complex mediated migration,(3) data for lesser nontransuranic isotopes such as ^{95}Zr and ^{93}Zr do not permit an absolute assessment of their importance in PWR waste, though it is a minor role.

STUDY OF MOBILITY CHARACTERISTICS OF ORGANIC COMPLEXES - J. A. Franz and Janet Russell

In an attempt to better characterize the state of polymerization of zirconium and niobium complexes of EDTA, tartrate and DTPA, nuclear magnetic resonance techniques (^{13}C, ^{91}Zr, and ^{93}Nb) were examined. ^{93}Nb Fourier transform nuclear magnetic resonance (FTNMR) at 19.443 MHz was attempted using tetrakis-(2,4-pentanedionato) zirconium (IV) in acetone-d_6. In both cases no signal within 16 kHz of the assigned frequencies could be detected using pulse repetition rates from 0.01 to 1.0 sec. It is apparent that even for these high-symmetry species quadrupole relaxation is very rapid, leading to T_1 values of $\sim 10^{-4}$ sec. For useful NMR spectra, line widths of observed transitions must be a fraction of the spectral width observed (800 Hz). Since line widths are equal to $1/\pi\ T_2$ or $1/\pi\ T_1$ (since $T_1 = T_2$), T_1 values should be $>10^{-3}$ sec. The planned study of T_1 *versus* state of polymerization thus was not feasible since T_1's of slowly rotating polymers of zirconium and niobium complexes are expected to have even shorter T_1's and thus not be observable due to very broad resonance lines.

EDTA and DTPA complexes of zirconium were reexamined to determine their solubility after previous studies with tartrate and gluconate complexes indicated that most soil tests would be conducted at below 10^{-4} $\underline{M}$. Both zirconium EDTA and DTPA were found to be soluble to the extent of 1×10^{-4} $\underline{M}$ and 3×10^{-4} $\underline{M}$. Since neither atomic absorption spectroscopy nor atomic emission spectroscopy was found to be sufficiently sensitive below these ranges, the ^{95}Zr-spiked complexes will be examined to augment previously examined tartrate and gluconate complexes.

In support of work with both zirconium and technetium, analytical procedures were further developed for monitoring ion exchange column effluents by combined NMR/liquid chromatography techniques. Detection of trace quantities of Zr:EDTA and Zr:DTPA complexes in the 10^{-4} $\underline{M}$ range was successfully carried out by ^{1}H FTNMR. Concentrations of organic complexes down to 10^{-6} $\underline{M}$ in D_2O are accessible by this technique, allowing monitoring of the liquid chromatography effluent from ion exchange columns for the separation of excess complexing agent from organic complexes. Figure 12.1 shows a ^{1}H NMR spectrum of 10^{-4} $\underline{M}$ Zr:DTPA in D_2O.

In previous work, characterization of ^{99}Tc:citrate complexes and ^{99}Tc:EDTA complexes has been solely by ultraviolet spectroscopy and electrophoresis.(4) This study's results will permit a much more detailed characterization of technetium complexes, including a correlation of the oxidation state of ^{99}Tc with NMR chemical shifts. The spectrum (Figure 12.1) of the zirconium complex is representative of use of the method, now underway, to characterize technetium complexes. This will permit a more detailed correlation of technetium complex structure with soil absorption characteristics.

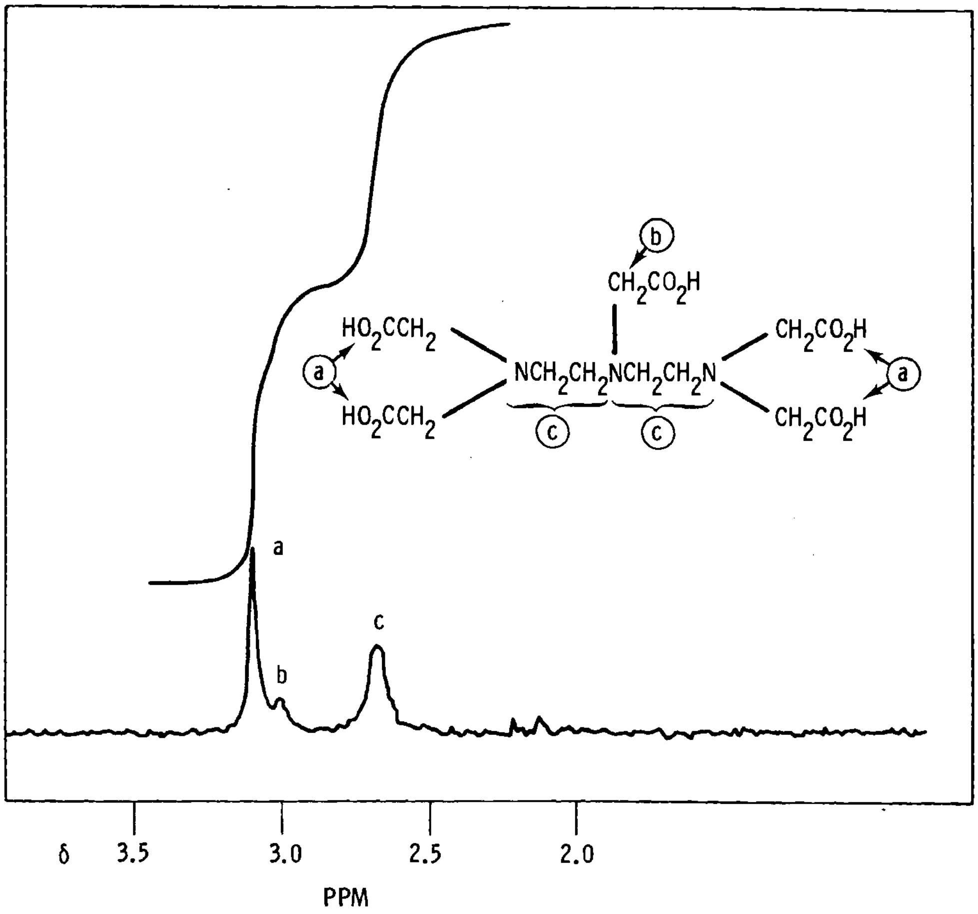

FIGURE 12.1. ^1H FTNMR Spectrum at 79.54 MHz of 1:1 Zr:DTPA Complex, 10^{-4} M in D_2O. The resonances labeled a, b, and c correspond to the ligand hydrogens indicated in the depicted structure (metal atom not shown for clarity). Chemical shifts are in parts per million (PPM) from external tetramethylsilane standard.

REFERENCES

1. Uri Gat, J. T. Thomas, and D. T. Clark, "Radioactive Waste Inventory at the Maxey Flats Nuclear Waste Burial Site." Health Physics, 30:281-289, 1975.
2. "Assessment of the Levels, Potential Origins and Transport Routes of the Radioactivity Measured in the Vicinity of the Maxey Flats Low-Level Radioactive Waste Disposal Site." Prepared for the Executive Department for Finance and Administration, Commonwealth of Kentucky, by Dames & Moore, March 1977.
3. J. L. Means, D. A. Crerar, and J. O. Duguid, "Migration of Radioactive Wastes: Radionuclide Mobilization by Complexing Agents." Science, 200:1477-1480, 1978.
4. R. Münze, "Zur Bildung Von Citratcomplexen des Technetiums." Radiochem. Radioanal. Letters, 30:61-64, 1977.

13.0 ELECTROPOLISHING FOR SURFACE DECONTAMINATION OF METALS

R. P. Allen and H. W. Arrowsmith - Project Managers

The objective of this program is to develop electropolishing as a large-scale decontamination technique for radioactive metal surfaces. Major program activities include 1) the establishment and operation of a demonstration decontamination facility and 2) laboratory studies to understand and optimize the decontamination process.

SUMMARY

The vibratory finisher was temporarily installed at the Hanford N-Reactor for intensive testing of its pretreatment capabilities. Results showed that use of the vibratory finisher rather than conventional chemical pretreatment methods not only reduced costs and personnel exposure, but also effectively removed gross contamination and concentrated the contamination in the sludge tank.

Other pretreatment studies have included evaluation of three chemical stripping compounds, which have shown promise in removing epoxy-type paints. In addition, epoxy paints and other tenacious surface materials have been removed using a high-pressure, liquid-plus-abrasive blaster.

Studies are under way to determine the effectiveness of prepolishing items that will become contaminated in their service environment. Scanning electron micrographs of the surfaces of as-received stainless steel bars show not only macroscopic irregularities but also a high density of submicron-size imperfections capable of entrapping contamination. Electropolishing removes essentially all these microscopic imperfections and rounds or smooths the large-scale surface irregularities.

DECONTAMINATION STUDIES

Decontamination studies have been hindered this quarter as a result of the accidental evaporation of nitric acid fumes into the electropolishing room. A heater in the rinse tank was left on over a weekend, resulting in significant corrosion damage to paint and nonstainless steel components. Cleanup operations have progressed satisfactorily, and full operation of the electropolishing facility is scheduled to resume soon.

PRETREATMENT STUDIES

Substantial progress has been made in further identifying and developing the sectioning and pretreatment techniques required to prepare contaminated material for final decontamination by electropolishing. A visit to the International Machine and Tool Show at Chicago, Illinois, resulted in identification of several types of shears, nibblers, and other types of metalworking machines capable of sectioning stainless steel with a minimum of waste and with a low probability of entraining surface contamination. A heavy-duty nibbler that can cut 0.25-in.-thick stainless steel at cutting speeds up to 6 ft/min has been ordered for evaluation.

The vibratory finisher was temporarily installed at the Hanford N-Reactor for intensive testing of its pretreatment capabilities using contaminated components generated by the reactor's summer outage. Results showed that the vibratory finisher is very effective in removing gross contamination and concentrating the contamination in a recently acquired sludge tank. For example, process tube end caps and inserts treated in the vibratory finisher (Figure 13.1) were decontaminated to 15 mR/hr compared to 245 mR/hr for inserts treated by regular chemical decontamination methods. Cost comparisons performed by United Nuclear Industries indicated that the use of vibratory finishing on process tube end caps and inserts could save over $8000/yr in their operations compared to regular chemical decontamination methods.

A 10% sodium hydroxide solution was used as the compound during these tests and was supplied at 7 gal/hr. The frequency of the vibration was 1200 vibrations/min and the amplitude was 0.25 in. A total of 30.6 ft^2 was processed in 30 hr, producing 1.4 ft^3 of waste. Items decontaminated included carbon steel process tube end caps and inserts (Figure 13.2), an

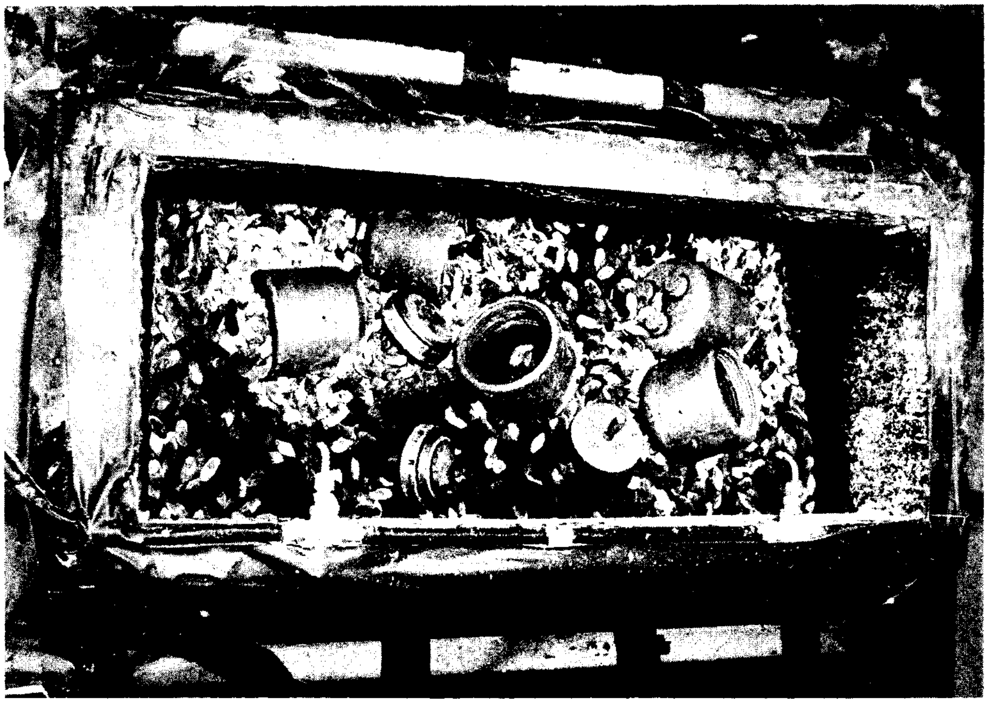

PNL 7807723-15

FIGURE 13.1. Process Tube End Caps and Inserts Being Processed in the Vibratory Finisher

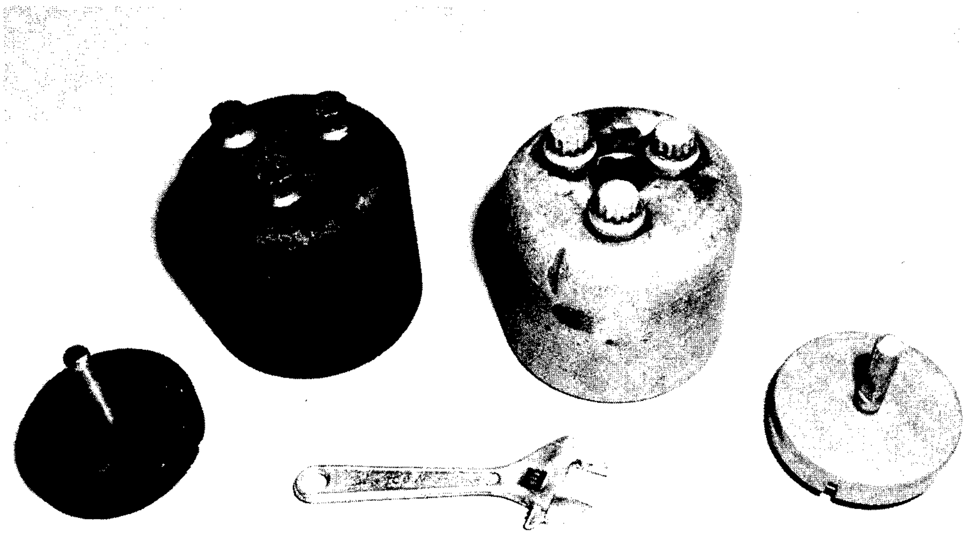

PNL 7807723-10

FIGURE 13.2. Before and After Comparison of Process Tube End Caps and Inserts Decontaminated in the Vibratory Finisher. Note that 12 end caps or 32 inserts can be processed in one batch.

electric pump motor housing (Figure 13.3), and various hand tools. The most dramatic reduction in radiation level occurred on an end cap--from 1.5 rad/hr to 200 mrad/hr in 4 hr processing time.

Another item processed was a ball channel inspection tool (Figure 13.4), constructed of stainless steel with rubber tubing covering about two-thirds of its length. Radiation levels on the tool were reduced from 1.5 rad/hr to 70 mrad/hr, with a 300-mrad/hr hot spot on the tubing. This was our first example of decontamination of a nonmetallic item by vibratory finishing.

The sludge tank, added to the compound handling system to facilitate removing secondary waste from the vibratory finisher, functioned effectively in these tests. This tank was double-lined with plastic sheets and positioned just behind the machine drain. A plastic pipe directed the effluent from the machine to the tank bottom. The liquid compound was skimmed from the surface through the sludge tank baffle device. It was then pumped by a plastic submergible pump through 5-μm filters and a flowmeter into the vibratory finisher bin. The sludge containing the radioactive contamination settled to the tank bottom and could be removed easily by lifting out the liner containing the waste.

Earlier studies have demonstrated the need to run the machine only when loaded to capacity to minimize waste generation since this is mainly a function of run time. Since the

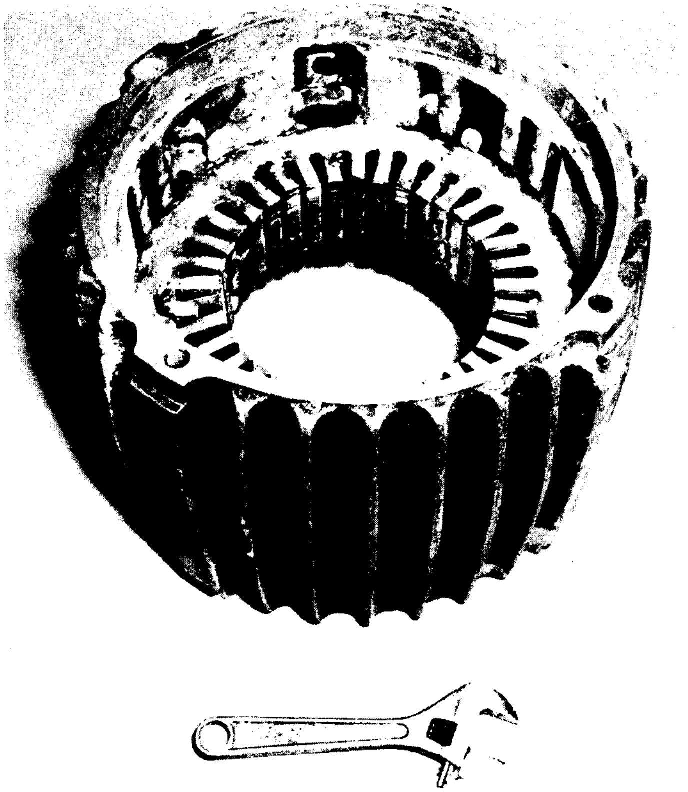

PNL 7807723-12

FIGURE 13.3. Electric Pump Motor Housing Decontaminated in the Vibratory Finisher During the N-Reactor Demonstration. (A 5-in. wrench has been added for size comparison.)

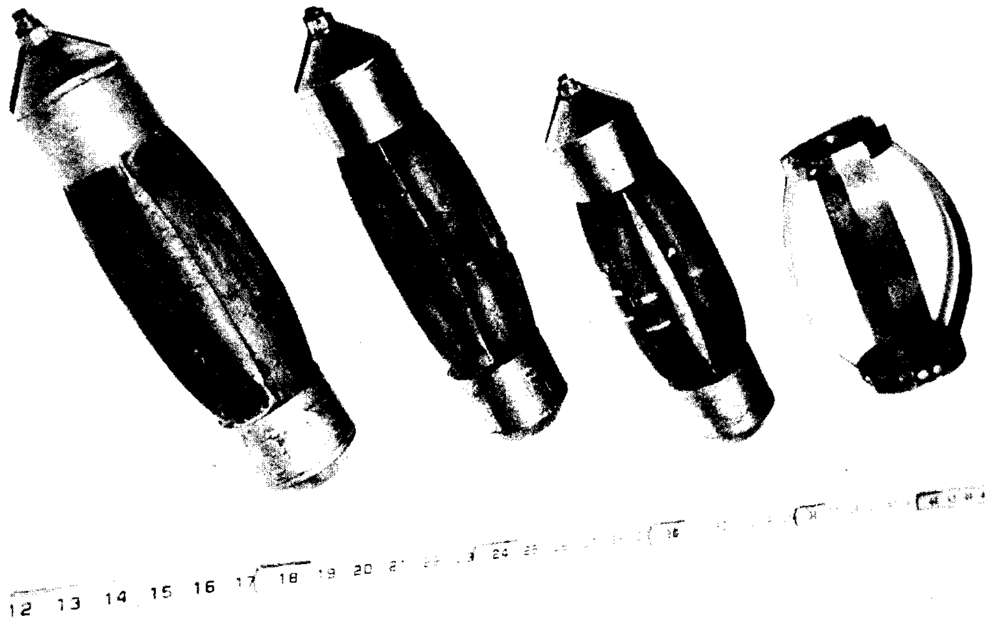

PNL 7808508-15

FIGURE 13.4. Ball Channel Inspection Tools Constructed of Stainless Steel and Rubber Tubing Decontaminated by Vibratory Finishing

vibratory finisher has been returned from Hanford N-Reactor, testing has been under way to determine the maximum surface area of material that can be effectively processed in the vibratory finisher. Results of this effort have shown that running a variety of sizes together (e.g., 4 x 24, 2 x 24, and 1 x 24 in. pieces) permits processing a higher volume of material with more effective results. To date a total of 61.1 ft^2 of stainless steel has been successfully processed at one time.

Three types of chemical stripping compounds are being evaluated as part of our pretreatment studies. These compounds have been tested on Amercoat® paint and Carbolene® (an epoxy-type paint) and will be tried on epoxy adhesives such as those used on glove box components from Rocky Flats. The most effective of the stripping compounds was a mixture of formic acid and methylene chloride. This compound, which would be suitable for use in an immersion tank, removed the Amercoat® in 4 min and the Carbolene® in 10 min.

In other pretreatment studies, a high-impact spray washer has been ordered, which operates at 250 psi and delivers 175 gal/hr. This washer can be used with hot chemical stripping compounds and also will be able to circulate chemical decontamination solutions for comparison studies.

Cold tests using a high-pressure, liquid-plus-abrasive blaster indicate that this also will be a very effective pretreatment method for removing epoxy paints and other tenacious surface material. The liquid blaster has been placed in the greenhouse in preparation for tests with contaminated material.

COMMERCIAL APPLICATIONS

Our electropolishing decontamination techniques are now being successfully applied by two commercial firms. These firms are offering to nuclear facilities electropolishing decontamination services designed to significantly reduce down-time and personnel exposure. They decontaminate such items as charging pumps, valves, tools, tubing, blades, and shipping casks. In addition, they are proposing the use of in-situ techniques on steam generators and heat exchangers.

PREPOLISHING STUDIES

Experience has shown that the surfaces produced by electropolishing are easier to clean using swab and other standard decontamination techniques than are metal surfaces with a normal as-received finish. The highly polished surface produced by the electropolishing treatment substantially reduces the time and radiation exposure required for subsequent decontamination using conventional techniques.

These observations suggest the use of electropolishing to prepolish the surface of items that become contaminated in their normal service environment to facilitate subsequent decontamination and possibly even to reduce the initial contamination level. This application of electropolishing should

---

® Registered trademarks of 1) Ameron, Inc., 201 North Berry St., Brea, CA, and 2) Carbolene Co., 350 Hanley Industrial Court, St. Louis, MO.

be useful for large components and surfaces such as shipping casks and refueling pool walls as well as for many types of smaller items, provided that the surfaces are not degraded by the service environment.

Prepolishing's effects on the decontamination behavior of metal surfaces can be understood qualitatively through comparing surface characteristics of typical as-received material with those of electropolished material. Figure 13.5 is a scanning electron micrograph of the surface of as-received 304L stainless steel bar with a hot-rolled, annealed and pickled (HRAP) finish. The HRAP surface shows the expected macroscopic irregularities, but most important from a decontamination standpoint are the high-density of submicron-size imperfections capable of entrapping and retaining contamination. Figure 13.6 shows the same surface material after electropolishing for 15 min in 85% H_3PO_4. The large-scale surface irregularities are still present, but rounded. However, the electropolishing treatment has removed essentially all the microscopic imperfections. Furthermore, the removal of these submicron imperfections occurs rapidly compared with the overall smoothing process. Figure 13.7 shows the surface produced by electropolishing the as-received material under the same conditions for only 5 min, corresponding to the removal of about 4 μm of metal. The microscopic imperfections have been eliminated, whereas general smoothing of the surface is just beginning.

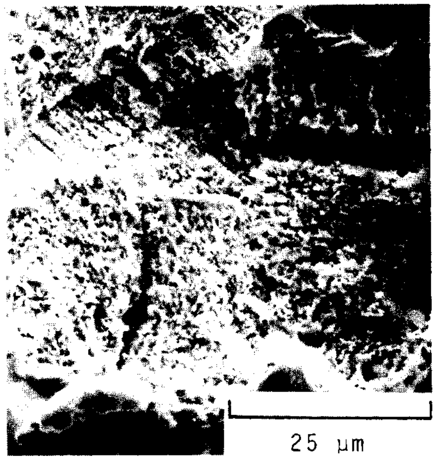

PNL 7804470-1

FIGURE 13.5. Scanning Electron Micrograph of an As-Received HRAP 304L Stainless Steel Surface Showing the High Density of Microscopic Surface Imperfections

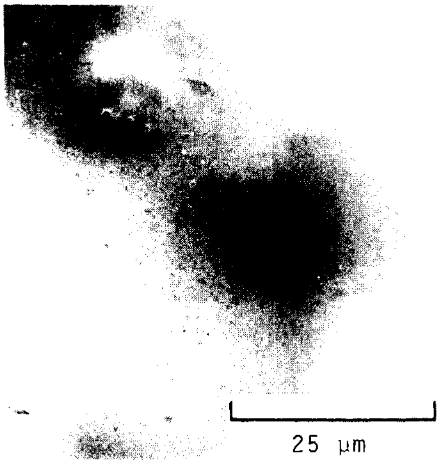

PNL 7804470-1

FIGURE 13.6. Scanning Electron Micrograph of 304L Stainless Steel Electropolished for only 15 min, Illustrating the Essentially Complete Removal of the Microscopic Surface Imperfections

Mechanically finished surfaces represent an intermediate case between mill and electropolished finishes with respect to density of microscopic imperfections. Figure 13.8, for example,

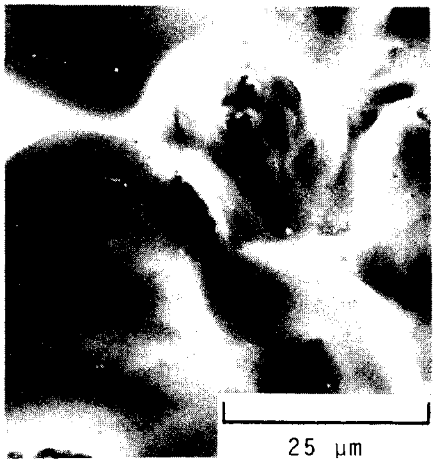

PNL 7804470-1

FIGURE 13.7. Scanning Electron Micrograph of 304L Stainless Steel Electropolished for only 5 min, Illustrating the Rapid Removal of the Microscopic Surface Imperfections

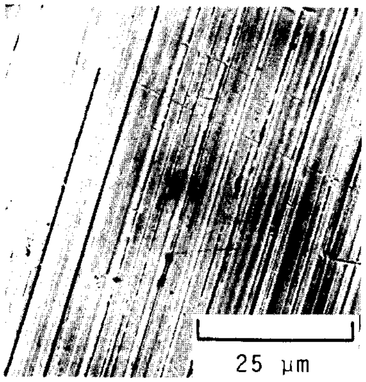

PNL 7804470-2

FIGURE 13.8. Scanning Electron Micrograph of 304L Stainless Steel Mechanically Ground to a No. 4 Finish, Producing a Flat Surface with a Moderate Density of Microscopic Imperfections

is a scanning electron micrograph of the surface produced by mechanically polishing 304L stainless steel to a No. 4 finish. Although the resulting surface is very flat and free of macroscopic irregularities, the scratches introduced by the grinding process are still potential traps for contamination. It should be noted, too, that the electropolished finish is both superior for decontaminating and usually much less expensive than a mechanically polished finish.

DISTRIBUTION

No. of
Copies

UNITED STATES

A. A. Churm
DOE Chicago Patent Group
9800 South Cass Avenue
Argonne, IL 60439

R. E. Cunningham
Deputy Director, Div. of Fuel
Cycle and Materials
Office of Nuclear Safety Materials
and Safeguards
Room 562
Nuclear Regulatory Commission
7915 Eastern Avenue
Silver Springs, MD 20910

J. Martin
Assistant Director for Radioactive
Waste Management Branch
NRC Division of Materials and
Fuel Cycle Facility Licensing
Washington, DC 20555

W. G. Belter
DOE Division of Biomedical and
Environmental Research
Earth Sciences Branch
Washington, DC 20545

W. A. Brobst
DOE Division of Environmental
Control Technology
Washington, DC 20545

W. E. Mott
DOE Division of Environmental
Control Technology
Washington, DC 20545

R. B. Chitwood
DOE Division of Nuclear Power
Development
Washington, DC 20545

T. C. Chee
DOE Office of Nuclear Waste Management
Washington, DC 20545

C. R. Cooley
DOE Office of Nuclear Waste Management
Washington, DC 20545

C. H. George
DOE Office of Nuclear Waste Management
Washington, DC 20545

C. A. Heath
DOE Office of Nuclear Waste Management
Washington, DC 20545

No. of
Copies

G. Oertel
DOE Office of Nuclear Waste Management
Washington, DC 20545

A. F. Perge
DOE Office of Nuclear Waste Management
Washington, DC 20545

D. L. Vieth
DOE Office of Nuclear Waste Management
Washington, DC 20545

R. D. Walton
DOE Office of Nuclear Waste Management
Washington, DC 20545

DOE Idaho Operations Office
PO Box 2108
Idaho Falls, ID 83401

J. Neff, Program Manager
Department of Energy
Columbus Program Office
505 King Avenue
Columbus, OH 43201

J. B. Whitsett
DOE Idaho Operations Office
PO Box 2180
Idaho Falls, ID 83401

John Van Cleve
Building 7601
Box X
Oak Ridge National Laboratories
Oak Ridge, TN 37830

334 DOE Technical Information Center

A. P. Roeh, Manager
Process Evaluation Branch
Allied Chemical Corporation
550 - 2nd Street
Idaho Falls, ID 83401

R. A. Brown
Allied Chemical Corporation
550 - 2nd Street
Idaho Falls, ID 83401

C. A. Hawley
Allied Chemical Corporation
550 - 2nd Street
Idaho Falls, ID 83401

D. A. Knecht
Allied Chemical Corporation
550 - 2nd Street
Idaho Falls, ID 83401

No. of
Copies

Allied Chemical Corporation
(File Copy)
550 - 2nd Street
Idaho Falls, ID 83401

G. W. Johnson
TRU Waste Management Program
DOE Albuquerque Operations Office
PO Box 5400
Albuquerque, NM 87115

J. A. Buckham
Allied-General Nuclear Services
PO Box 847
Barnwell, SC 29812

A. Williams
Allied-General Nuclear Services
PO Box 847
Barnwell, SC 29812

J. L. Jardine
Argonne National Laboratory
9700 South Cass Avenue
Argonne, IL 60439

M. J. Steindler/L. E. Trevorrow
Argonne National Laboratory
9700 South Cass Avenue
Argonne, IL 60439

Battelle Memorial Institute
505 King Avenue
Columbus, OH 43201

J. M. Batch
Battelle Project Management
Division
Battelle Memorial Institute
505 King Avenue
Columbus, OH 43201

H. C. Burkholder
Battelle Project Management
Division
Battelle Memorial Institute
505 King Avenue
Columbus, OH 43201

R. E. Heineman
Battelle Project Management
Division
Battelle Memorial Institute
505 King Avenue
Columbus, OH 43201

2 Brookhaven National Laboratory
Reference Section
Information Division
Upton, Long Island, NY 11973

No. of
Copies

Combustion Division
Combustion Engineering, Inc.
Windsor, CT 06095

Lawrence J. Smith
TRU Waste Systems Office
Bldg. T-790
Rockwell International
Rocky Flats Plant
PO Box 464
Golden, CO 80401

E. Vejvoda, Director
Chemical Operations
Rockwell International
Rocky Flats Plant
PO Box 464
Golden, CO 80401

M. D. Boersma
duPont Company, Aiken (DOE)
E. I. duPont deNemours & Co.
Savannah River Laboratory
Aiken, SC 29801

C. H. Ice
duPont Company, Aiken (DOE)
E. I. duPont deNemours & Co.
Savannah River Laboratory
Aiken, SC 29801

A. S. Jennings
duPont Company, Aiken (DOE)
E. I. duPont deNemours & Co.
Savannah River Laboratory
Aiken, SC 29801

R. Maher
duPont Company, Aiken (DOE)
E. I. duPont deNemours & Co.
Savannah River Laboratory
Aiken, SC 29801

P. H. Permar
duPont Company, Aiken (DOE)
E. I. duPont deNemours & Co.
Savannah River Laboratory
Aiken, SC 29801

L. Henning
Electric Power Research Institute
3412 Hillview Avenue
PO Box 10412
Palo Alto, CA 94304

Environmental Protection Agency
Technology Assessment Division
(AW-559)
Office of Radiation Programs
U.S. Environmental Protection
Agency
Washington, DC 20460

No. of
Copies

R. G. Barnes
General Electric Company
175 Curtner Avenue
(M/C 160)
San Jose, CA 95125

L. H. Brooks
Gulf Energy and Environmental Systems
PO Box 81608
San Diego, CA 92138

2 Central Research Library
Document Reference Section
Oak Ridge National Laboratory (DOE)
Oak Ridge, TN 37830

3 Los Alamos Scientific Laboratory
PO Box 1663
Los Alamos, NM 87544

C. J. Kershner
Monsanto Research Corporation
Mound Laboratory
PO Box 32
Miamisburg, OH 45342

John Pomeroy
Technical Secretary
National Academy of Sciences
Committee of Radioactive Waste Management
National Research Council
2101 Constitution Avenue
Washington, DC 20418

2 J. P. Duckworth
Plant Manager
Nuclear Fuels Services, Inc.
PO Box 124
West Valley, NY 14171

J. L. Larocca, Chairman
Engineering Research and Development Authority
Empire State Plaza
Albany, NY 12223

D. R. Anderson
Sandia Laboratories
Albuquerque, NM 87115

W. Weart
Division 1140
Sandia Laboratories
Albuquerque, NM 87115

O. E. Jones
Sandia Laboratories
Albuquerque, NM 87115

No. of
Copies

J. W. Bartlett
The Analytical Sciences Corp.
6 Jacob Way
Reading, MA 01867

R. E. Blanco
Union Carbide Corporation (ORNL)
Chemical Technology Division
PO Box Y
Oak Ridge, TN 37830

J. O. Blomeke
Union Carbide Corporation (ORNL)
Chemical Technology Division
PO Box Y
Oak Ridge, TN 37830

2 D. E. Ferguson
Union Carbide Corporation (ORNL)
Chemical Technology Division
PO Box Y
Oak Ridge, TN 37830

A. L. Lotts
Union Carbide Corporation (ORNL)
Chemical Technology Division
PO Box Y
Oak Ridge, TN 37830

W. C. McClain
Union Carbide Corporation (ORNL)
Chemical Technology Division
PO Box Y
Oak Ridge, TN 37830

R. A. Beall
U.S. Department of Interior
Bureau of Mines
Albany Research Center
1450 W. Queen Avenue
Albany, OR 97321

R. G. Post
College of Engineering
University of Arizona
Tucson, AZ 85721

FOREIGN

2 International Atomic Energy Agency
Kärtner Ring 11
PO Box 590
A-1011, Vienna, AUSTRIA

Rene Amavis
Euratom
Health Physics Division
29, Rue Aldringer
Luxembourg, BELGIUM

No. of
Copies

S. Orlowski
Commission of the European
Communities
Rue de la Loi 200
B-1049 Brussels, BELGIUM

M. Tomlinson
Director of Chemistry and Materials
Science Division
Atomic Energy of Canada, Ltd.
Whiteshell Nuclear Research
Establishment
Pinawa, Manitoba, CANADA

K. D. B. Johnson
Atomic Energy Research
Establishment
Harwell, Didcot,
Berks, ENGLAND

D. W. Clelland
United Kingdom Atomic Energy
Authority
Risley, ENGLAND

P. J. Regnaut
Centre d'Etudes Nucléaires
de Fontenay-aux-Roses
Boite Postale 6
92 - Fontenay-aux-Roses
FRANCE

Y. J. Sousselier
Centre d'Etudes Nucléaires
de Fontenay-aux-Roses
Boite Postale 6
92 - Fontenay-aux-Roses
FRANCE

Bundesministerium für Forschung
und Technologie
Stressemannstrasse 2
5300 Bonn
GERMANY

Hans W. Levi
Hahn-Meitner-Institut
für Kernforschung
Glienicker Strasse 100
1000 Berlin 39
GERMANY

Center for Atomic Energy
Documentation (ZAED)
Attn: Dr. Mrs. Bell
PO Box 3640
7500 Karlsruhe
GERMANY

No. of
Copies

H. Krause
Kernforschungszentrum Karlsruhe
GmbH (KfK)
Postfach 3640
D7500 Karlsruhe
GERMANY

N. S. Sunder Rajan
Bhabha Atomic Research Centre
Waste Treatment Division
Trombay, Bombay, 400 085 INDIA

R. V. Amalraj
C.W.M.F. Project
P.O. Kalpakkam
Chingleput Dist.
Tamil Nadu, INDIA

ONSITE

9 DOE Richland Operations Office

E. A. Bracken
J. A. Fernandez
R. E. Gerton
R. B. Goranson
H. E. Ransom
J. J. Schreiber
M. W. Shupe
M. J. Zamorski
O. J. Elgert

11 Rockwell Hanford Operations

H. Babad
L. C. Brown
R. A. Deju
R. J. Gimera
D. R. Gustavson
E. J. Kosiancic
C. M. Manry
I. E. Reep
J. H. Roecker
D. D. Wodrich
File Copy

Exxon
Richland, WA 99352

S. J. Beard

Joint Center for Graduate Study

J. Cooper

United Nuclear Industries, Inc.

T. E. Dabrowski

No. of Copies	
	Westinghouse Hanford Company
	A. G. Blasewitz
57	Pacific Northwest Laboratory
	R. P. Allen/H. W. Arrowsmith
	T. W. Ambrose
	N. E. Ballou
	A. Brandstetter
	R. L. Brodzinski
	L. L. Burger
	N. E. Carter
	D. B. Cearlock
	T. D. Chikalla
	M. O. Cloninger
	R. L. Dillon
	P. G. Doctor
	J. R. Eliason
	J. W. Finnigan
	J. C. Fox
	J. A. Franz
	J. J. Fuquay
	G. W. Gee
	R. W. Goles
	B. Griggs
	A. J. Haverfield
	J. L. Hooper
	E. R. Irish

No. of Copies	
	J. H. Jarrett
	R. S. Kemper
	M. R. Kreiter
	L. T. Lakey
	T. M. Lambright
	J. M. Latkovich
	I. S. Levy
	R. C. Liikala
	R. P. Marshall
	J. L. McElroy
	R. D. Nelson
	J. M. Nielsen/R. W. Perkins
	R. E. Nightingale
	D. E. Olesen
	C. R. Palmer
	A. M. Platt
	J. A. Powell
	J. V. Robinson
	C. L. Simpson/C. E. Elderkin
	G. L. Tingey
	C. M. Unruh
	H. H. Van Tuyl
	J. W. Voss
	E. J. Wheelwright
	W. R. Wiley
	L. D. Williams
	W. K. Winegardner
	Technical Information (5)
	Publishing Coordination (2)